

Secondary Organic Aerosol Particles from Southern Finland, Amazonia, and**California Studied by Coherent Vibrational Spectroscopy**

Carlena J. Ebben,¹ Mona Shrestha,¹ Imee S. Martinez, Ashley L. Corrigan,² Amanda A. Frossard,² Wei W. Song,³ David R. Worton,⁴ Tuukka Petäjä,⁵ Jonathan Williams,³ Lynn M. Russell,² Markku Kulmala,⁵ Allen H. Goldstein,⁴ Paulo Artaxo,⁶ Scot T. Martin,⁷
Regan J. Thomson,¹ and Franz M. Geiger^{1*}

¹*Department of Chemistry, Northwestern University, 2145 Sheridan Road, Evanston, IL 60208, USA;* ²*Scripps Institution of Oceanography and the University of California, San Diego, La Jolla, CA 92093, USA;* ³*Max Planck Institute for Chemistry, 55128 Mainz, Germany;* ⁴*Department of Civil and Environmental Engineering, University of California, Berkeley, CA, 94720;* ⁵*Department of Physics, FI-00014 University of Helsinki, Finland;* ⁶*Institute of Physics, University of São Paulo, Rua do Matão, Travessa R, 187, 05508-090, São Paulo, Brazil;* ⁷*School of Engineering and Applied Sciences & Department of Earth and Planetary Sciences, Harvard University, 29 Oxford Street, Cambridge, MA 02138, USA.*

Abstract. This Article summarizes and compares the analysis of natural aerosol particles from three different forest environments by vibrational sum frequency generation. The experiments were carried out directly on filter and impactor substrates, without the need for sample pre-concentration, manipulation, or destruction. We discuss the important first steps leading to SOA particle nucleation and growth from α -pinene by showing that, at least as viewed by vibrational coherent spectroscopy, the chemical composition is close to size-invariant over the size range studied here. We also introduce the concept of

molecular chirality as a chemical marker that could be useful for quantifying how chemical constituents in the SOA gas phase and the SOA particle phase are related in time. In addition, we show how micrograms of SOA particle material on a collection filter are readily analyzed by vibrational sum frequency spectroscopy in a non-destructive fashion that does not require pumping on the sample. Finally, we describe how the combination of multiple disciplines, such as aerosol science, advanced vibrational spectroscopy, meteorology, and chemistry can be highly informative when studying particles collected during atmospheric chemistry field campaigns, such as those carried out during AMAZE-08, HUMPPA-COPEC-2010, or BEARPEX, and when they are compared to results from synthetic model systems such as the Harvard Environmental Chamber. Discussions regarding the future of SOA chemical analysis approaches are provided in the context of providing a path towards detailed spectroscopic assignments of SOA particle precursors and constituents and to fast-forward, in terms of mechanistic studies, through the SOA particle formation process.

*Corresponding author

Keywords. Secondary organic aerosol particles, α -pinene, isoprene, vibrational sum frequency generation, biogenic volatile organic compounds, coherent spectroscopy.

I. Introduction. The 2007 IPCC Report states that the roles of aerosols in the climate system "*remain the dominant uncertainty in radiative forcing.*"¹ Despite this prominent role, the level of scientific understanding regarding aerosols has been rated "very low" for close to a decade,^{1,2} contributing significantly to the large (>50%) uncertainty associated with the net anthropogenic radiative forcing estimates that range from +0.6 to 2.4 W m⁻². Of particular importance are secondary organic aerosol (SOA) particles, whose formation can be associated with the emission of biogenic volatile organic compounds (BVOCs) from the Earth's large forest systems, some of which range from continental to global spatial scales (Fig. 1A). The boreal forests, for instance, spans more than twelve time zones on the northern hemisphere, while the tropical forests span roughly one third to half of the equator. To provide a scale of the impact that SOA particles formed from BVOCs emitted from forests can have on the climate system, we point out that SOA production over the Finnish boreal forest results in up to -14 Wm⁻² radiative forcing, compared to a global mean of up to -1.1 Wm⁻².³ The strong positive temperature dependence of BVOC emissions⁴⁻⁶ is likely to increase the importance of SOA particles under future – possibly warmer – climates,⁷ provided that higher BVOC concentrations coincide with higher SOA particle concentrations.

While SOA particle formation in particular ranks among the least understood atmospheric processes in the climate system,⁸⁻¹² molecular studies linking BVOC emissions to the aerosol particle phase¹³⁻¹⁶ have identified relevant reaction pathways that begin with oxidation, such as ozonolysis of a C=C double bond.¹⁷⁻¹⁹ In the case of the ozonolysis of α -pinene, the most commonly found terpene in boreal forests, this processes leads to the formation of less-volatile organic compounds, such as

pinonaldehyde and pinonic acid. Dimerization and oligomerization processes have been reported to be important as well,²⁰⁻²³ along with the formation of pinic acid and terpenylic acid.²⁴ Likewise, the oxidation of isoprene, which is the dominant plant emission in tropical forests, has been reported to involve species such as epoxides, which also exhibit lower volatility.^{25,26} The lower vapor pressures of the oxidized compounds²⁷⁻³⁰ can lead to their condensation, ultimately producing SOA particles.²⁰⁻²³

Many of the implicated reactions involve condensations between the various reactive and stable species that are produced from the photochemical oxidation and ozonolysis of C=C double bonds present within biogenic terpenes. For instance, Kroll and Seinfeld²⁸ proposed that the formation of peroxyhemiacetals, hemiacetals, sulfate esters, adducts of stable Criegee intermediates, anhydrides, and aldol products may occur under tropospheric conditions, however, the mechanisms of these proposed reaction pathways have not yet been tested in a systematic fashion. This is in part due to the difficulty in carrying out the chemical analysis of SOA particles, especially if one wishes to study them with non-destructive methods that are applicable under ambient pressure and temperature conditions. Within this context, we believe that physical chemists are confronted with the following four research challenges: i) while vitally needed for improving computer modeling efforts aimed at quantitatively predicting SOA yields for a given atmospheric gas phase composition,¹² the molecularity of even the first few reactions leading to SOA particle formation is not known; ii) given a lack of chemical markers that are needed for quantifying how chemical constituents in the SOA gas phase and the SOA particle phase are related, time constants for SOA formation from terpene-rich air are not known; iii) the chemical analysis of SOA particles is difficult to carry out

with non-destructive methods that are applicable at ambient pressure and temperature; and iv) the expertise for SOA particle sampling is typically not found in chemistry departments but rather in atmospheric science and chemical engineering departments, requiring students to master multiple disciplines.

In this Feature Article, we address these four points by relating (i) how we connected with established field and laboratory projects studying SOA particles, (ii) how we applied coherent vibrational spectroscopy to SOA particles for the first time, and (iii) what we learned from our spectroscopic studies in terms of SOA particle formation. We summarize and compare our results from the application of coherent vibrational spectroscopy to aerosol particles collected in the central Amazon Basin, chosen as an example of a tropical forest, in Southern Finland, chosen as an example of the boreal forest, and in Blodgett Forest, California, an anthropogenically influenced ponderosa pine forest. Tropical forest air is typically rich in isoprene, whereas air over the boreal and the pine forests is typically rich in α -pinene, and we expect the vibrational spectra obtained from the particles to be due to oxidation products of these compounds in the particles phase. By working with the Harvard Environmental Chamber,³¹ which has now become a major synthetic facility for preparing organic aerosol particles under tropospherically relevant reactant partial pressure conditions, we compare the results from the natural samples with those obtained from synthetic model systems. We learn from our studies that SFG spectroscopy can provide a substantial sensitivity advantage over other non-destructive methods that can be performed under ambient temperature and pressure conditions, and that SFG is most informative when it is combined with the full range of aerosol particle and gas phase analytics that is emblematic of atmospheric chemistry field

campaigns such as AMAZE-08,³² HUMPPA-COPEC-2010,³ or BEARPEX.³³

II. Organization. Prior to describing our findings and discussing the results, we provide here an overview of the organization of this Feature Article. We begin in section II with the description of the three field measurement sites where the particles studied here were collected. Section IV and V continue with a discussion of the standard methods for aerosol particle collection, synthesis, sizing, and chemical analysis. As the particle collection methods available at the field sampling sites were not identical, the purpose of the section on particle collection and analytics (sections IV and V) is to provide details of the instrumentation that was used to collect and analyze the aerosol particle material at each site. Section V also contains a section on aerosol particle synthesis for laboratory modeling studies that can be used to interpret results obtained from the field-derived particles. Section VI provides an overview of the coherent vibrational spectroscopy used to analyze the aerosol particle phase, and section VII provides results regarding synthetic modeling studies carried out at the Harvard Environmental Chamber. The results from the field-derived particles are discussed in sections VIII-X, and section XI summarizes this work.

III. Aerosol Particle Sampling Locations. The boreal forest field site we worked with during the summer of 2010³ is located at the Station for Measuring Forest Ecosystem-Atmosphere Relations (**SMEAR II**) at Hyytiälä (61°51' N, 24°17' E) in Southern Finland (Fig. 1B, left panel). The site is 230 km north of Helsinki, 170 m above sea level (asl) and surrounded by boreal forest. The predominant tree species is scots pine (*Pinus sylvestris*) with some spruce (*Picea abies*), aspen (*Populus sp.*) and birch (*Betula sp.*). Anthropogenic influences at the site are generally low, particularly when the wind comes

from the sparsely populated northern sector. Incidental pollution from forest management activities and minor traffic did occur during the field intensive and was readily identified by aromatic compounds such as toluene and benzene in the gas phase. A 120 m tall tower was used for measurements of meteorological, physical, and chemical parameters at various heights above the 16 m canopy top. The relevant meteorological conditions for the site are listed in Table I, which also shows that the oxidative chemistry is driven mainly by ozone.

The tropical forest field site is located at tower TT34,³² which is situated within a pristine terra firme rainforest in the Reserva Biologica do Cuieiras and managed by the Instituto Nacional de Pesquisas da Amazonia (INPA) and the Large-Scale Biosphere-Atmosphere Experiment in Amazonia (LBA), 60 km NNW of downtown Manaus (Fig. 1B, right panel). The forest canopy height near the tower varies between 30 and 35 m; the sampling height on the tower is 38.75 m. Andreae et al.³⁴ summarized meteorological and climatological information and some of the relevant data for the period of study are summarized in Table I. Briefly, VOC emissions in the Amazon Basin are the Earth's largest³⁵⁻³⁷ and far outweigh anthropogenic emissions. Along with a high solar flux, there is a large source of OH radicals in the gas phase,³⁸ which dominates SOA production chemistry. In contrast, SOA production due to reactions involving ozone is less important due to relatively low ozone concentrations (5 to 20 ppb). Overall, the central Amazon represents a pristine environment that is characterized by having nearly pure biogenic aerosol particles during the wet season (October through March).³⁹⁻⁴⁴ Specifically, up to 90% of the atmospheric particles sampled in the fine mode (size less than 1 micron) were composed of SOA particles formed by atmospheric oxidation and gas-to-particle

conversion of BVOCs, and no other chemical components were present in these particles within the limit of detection. This characteristic makes the area an ideal natural laboratory to isolate natural SOA production and thereby provide a baseline understanding against which to measure anthropogenic influences.

Finally, we also studied particles collected during the Biosphere Effects on AeRosols and Photochemistry EXperiment (BEARPEX)³³ 2009 Campaign in Blodgett Forest, which is a ponderosa pine (*Pinus ponderosa*) forest, located in the foothills of the Sierra Nevada Mountains of Northern California (38° 59' N, 120° 58' W, Fig. 1B, center panel) at an elevation of 1315 m. This site has a Mediterranean climate, with very little precipitation during the summer months. The typical daytime air mass trajectory is from the southwest, from the populated Sacramento Valley, while at night the most common trajectory is from the Sierra Nevada Mountains northeast of the site.^{33,45} Depending on the origin of air masses arriving at the site, there is the potential for significant anthropogenic influence in the formation of secondary organic particle material. Some of the relevant conditions are summarized in Table I.

IV. Collection of Aerosol Particles. In general, the collection of aerosol particles is carried out such that various aerodynamic size ranges are sampled in order to evaluate particles in the fine (<1 μm) and coarse (>1 μm) modes. Particulate matter with sizes below 1 μm (PM1) can be collected selectively by using a cyclone. At Northwestern, we recently built a PM1 particle sampler that is based on such a device (Fig. 2A). This sampler consists of a PM1 cyclone (URG Corporation, part #: URG-2000-30EHB), which is connected to a flow splitter (Brechtel Manufacturing Inc., model 1102). A flow of approximately 5.1 slpm is directed through a 47 mm closed aluminum filter holder

(BGI Incorporated, part #: F1) and is controlled by a mass flow controller (MKS, part #: m100b14cs1bn--s). The rest of the flow, approximately 11.6 slpm, passes through a bypass line. A HEPA capsule (Pall Life Sciences, part #: 28145-145) is placed before a vacuum pump, which pulls flow through the system. Particles are collected on Teflon filters (Pall Life Sciences, 47 mm diameter, 1 μ m pore size, part #: 28139-125) and kept in a freezer until analysis.

More sophisticated approaches employ the use of micro-orifice uniform-deposit impactors (MOUDI, Fig. 2B),⁴⁶ which can yield highly size-resolved particle samples down to ten nanometers, depending on the model. Particle sizing within a MOUDI is subject to log-normal size distributions, and when several sizes are collected simultaneously on several stages, some spill-over of larger particles onto a stage sampling particles with smaller sizes can occur. Sampling methods using a PM1 sampler or a MOUDI result in low loadings of particles, typically corresponding to a mass of a few micrograms or less on a given filter or stage, which are distributed over a one-inch diameter surface. Therefore, the analysis of aerosol particles collected in such a fashion represents a classical 'detection limit' problem for some situations and curtails the analysis of particles collected over short times or the analysis of particles present at low concentrations in the air at the time of collection.

V. Aerosol Particle Analytics. To fully understand the role that secondary organic aerosol particles play in our climate system, several properties of the particles are needed, including size, hygroscopicity, CCN activity, and chemical composition. A wide range of analytical tools have been developed and repeatedly improved upon to determine these

properties. Use of a combination of these tools is nearly always the best way to obtain a cohesive picture of SOA properties.

A. Particle Sizing. One of the most sought-after physical properties of aerosol particles is their size distribution and its link to the direct and indirect effect of radiative forcing.⁴⁷ Particle size distributions are determined using a variety of measurement techniques. One of the most common methods is a differential mobility particle sizer (DMPS), which is made up of a differential mobility analyzer (DMA) and a condensation particle counter (CPC). Particles are size-selected according to their mobility in an electric field in the DMA, and those that pass through the DMA are counted in the CPC. The DMPS has been widely used in determining growth rates of particles following new particle nucleation events.⁴⁸ This method is advantageous in that it allows particles of a wide range of sizes to be analyzed; however, one shortcoming of the DMPS is that particles of only a small size range can be sampled during each scan. To obtain a full size distribution, several size fractions must be analyzed, and this binning procedure leads to limited temporal resolution. The temporal resolution may be improved by using a scanning mobility particle sizer (SMPS), which scans through a range of voltages in the DMA in order to quickly obtain a full particle size distribution. Studies involving SMPS measurements are generally carried out at 90% RH, to allow for intercomparison between measurements; however, this prevents analysis of the deliquescence behavior of particles.⁴⁹ For both the DMPS and SMPS, multiple charging on particles and non-spherical particle shapes may lead to inaccuracies in sizing. These mobility sizing techniques offer lower detection limits than optical particle counters (OPCs), which may not be able to detect particles smaller than about 50 nm. A second advantage of mobility

sizing is that uncertainty in particle refractive index does not impact sizing as it does for the OPC.⁵⁰

Particle size measurements are also important for understanding and predicting aerosol particle nucleation events. Instruments such as the DMPS and SMPS have been valuable in studying such events, but these methods generally have detection limits of 3 nm particles or larger. Because of this detection limit, concentrations of the smallest particles are inferred based on the flux of new particles into the measurable size range, rather than being measured directly. The balanced scanning mobility analyzer (BSMA) may be used to improve characterization of the smallest molecular clusters and particles.^{51,52} The air ion spectrometer (AIS)^{53,54} and neutral cluster and air ion spectrometer (NAIS)⁵⁵⁻⁵⁷ also allow for the detection of particles below 2 nm. Issues with the variety of instruments used for particle sizing include differences in the parameters used to determine particle size between techniques, as well as differences in resolution and accuracy of measurements.⁵⁸ These inconsistencies complicate the comparison of particle size distributions obtained using different measurement techniques.

B. Hygroscopicity and Cloud Condensation Nuclei Activity. The hygroscopicity parameter, κ , is related to Köhler Theory, which uses the physicochemical properties of particles to predict their CCN activity.⁵⁹ Assuming values for the surface tension of water and the density of the SOA particle material,^{60,61} one can estimate the average molecular weight of a particle composed of purely secondary organic material. The hygroscopicity parameter can also be used to draw conclusions regarding the class of compounds making up particles, since marine aerosol particles typically have a higher κ value than terrestrial particles, and inorganic terrestrial particles have a higher κ value than organics or dust,

which take up very little water. Analysis of particle hygroscopicity is used to relate chemical composition to CCN activity.^{59,62-64}

A cloud condensation nuclei counter (CCNC) is used to determine the κ value of particles.⁶⁵ In this technique, particles are exposed to a supersaturated environment. By changing the supersaturation and counting the particles that activate at each supersaturation, the CCN activity of particle samples can be investigated. Use of the CCNC in conjunction with a DMA allows for the determination of CCN activity as a function of particle size. One shortcoming of the CCNC is that assumptions must be made in determining which supersaturated particles exiting the CCNC are activated, and often thermodynamic models must be used to aid in this determination.⁶⁶

The hygroscopic tandem differential mobility analyzer (HTDMA) may also be used to gain some insight into particle hygroscopicity and CCN activity.⁶⁷ This instrument uses two DMAs in parallel; the first selects particles in a certain size range. These particles pass through a humidifier, where they undergo condensational growth, then through a second DMA to determine the growth factor associated with humidification. The relative growth of the particles through the uptake of water can be related to their chemical composition.⁶⁸ It should be noted that the accuracy of these measurements relies on the very precise control of temperature and relative humidity in the second DMA.^{68,69} While CCNC and HTDMA measurements provide beneficial information on particle hygroscopicity and CCN activity, definitive conclusions regarding the chemical composition of individual particles may not be drawn from these analyses.

C. Chemical Composition of Secondary Organic Aerosol Particles.

1. On-line Analysis. Much of the chemical analysis of natural and synthetic SOA particles to date has been carried out using mass spectrometry.⁷⁰⁻⁷⁴ The aerosol mass spectrometer (AMS)⁷⁵ has been the workhorse in the field, and high-resolution time of flight mass spectrometry (HR-ToF-MS) has been the preferred laboratory approach. Benefits of mass spectrometry include the ability to assess the size and chemical composition of single particles in real time, eliminating the possibility of artifacts or loss of volatile species that can be problems in offline analysis. The interpretation of mass spectra obtained from natural or synthetic SOA particles is based on data obtained from highly complex mixtures, which has made the process of deconvoluting the underlying molecular structures of the particle constituents challenging. For instance, the Johnston group attributed MS fragmentation patterns from SOA particles that might be derived from α -pinene aldol adducts,^{76,77} but confirmation of these assignments has yet to occur. Little concrete evidence for chemical structures is available, mainly because reference compounds for benchmarking and chemical identification do not exist. An important collection of data that are available, however, is the oxygen-to-carbon (O/C) ratio of various SOA particles.⁷⁸ The O/C ratios report on the oxidation state of the aerosol particle constituents, and they have been used to determine the sources of these constituents. O/C ratios often provide insight into the age of particles, since the O/C ratio of a particle typically increases as it becomes more processed.⁷⁹ By working with major field campaigns, we recently reported that SOA particles from air rich in α -pinene, such as those from Southern Finland, have O/C ratios between 0.5–0.7, whereas isoprene-rich samples from the central Amazon Basin have O/C ratios between 0.3–0.5.⁸⁰ Other

complex field-obtained mixtures of various forms of organic aerosol particles can have O/C ratios as low as below 0.1 and as high as 0.8 (Table I).⁷⁸

Particles synthesized in a laboratory under controlled conditions are often used to benchmark results obtained from more chemically complex particles collected during field studies. Particles synthesis may take place in a flow tube or a cloud chamber, and the particles are generally evaluated by mass spectrometry, sizing techniques, and other online analyses, as well as offline techniques. The major difference between flow tube and chamber approaches is in the concentration of oxidant and precursor used to synthesize the particles. Specifically, while chamber experiments take far longer to complete, the oxidant and monoterpene concentrations utilized are generally more relevant to atmospheric conditions. Looking at, for example, the ozonolysis of monoterpenes in a chamber, ozone concentrations typically fall in the range of 50 ppb to 1 ppm, while typical monoterpene concentrations are 1-300 ppb.⁸¹⁻⁸⁸ Flow tube experiments are beneficial in that they may be completed quickly; however, they are often carried out at very high concentrations, which may produce particles that are formed under conditions that are not of direct atmospheric relevance. While this is a concern when comparing the results of flow tube studies to field collected data, flow tube studies allow for the fast screening of reaction conditions and resultant aerosol particle properties. In flow tube studies, typical ozone concentrations are 100 ppb to 1 ppm, similar in concentration to chamber studies, although George et al. used ozone concentrations as high as 75 ppm.⁸⁹ Monoterpene concentrations, however, may be several orders of magnitude higher in concentration than used in a chamber, typically in the range of 0.4 to 300 ppm.^{30,76,89-93}

2. Off-line Analysis. Off-line measurements fill important gaps in the characterization of SOA particles. Thermal desorption (TD) may be used to determine the chemical composition of particle samples.^{94,95} Particles are collected onto a substrate, which is then heated in a very controlled manner. Solid or liquid components are released into the gas phase based on their volatility and are analyzed using mass spectrometry. The temperature can also be slowly raised, as in temperature programmed thermal desorption, and the intensities of m/z ratios of interest may then be measured as a function of temperature. Ziemann and coworkers have had much success using TPTD to obtain mass spectra of particles from chamber studies.^{96,97} Versus offline methods of analysis which use solvent extraction, TD has high sensitivity allowing for shorter sample collection times, and there is also a smaller probability of sample contamination.⁹⁸ In addition, TD analysis may be extended to organic compounds that are insoluble in the solvents commonly used for extraction. However, due to the high temperatures used for vaporization of samples, some substrates, such as Teflon, may become unstable and cannot be used to collect samples. Some organic compounds are also thermally labile, and these may undergo chemical changes or degradation during vaporization, impacting their characterization by TD. TD is also more suitable for the analysis of non-polar organics than for polar compounds such as carboxylic acids.⁹⁹ Compounds with similar volatilities are difficult to characterize using TD-MS; however, separation of these compounds by the use of TD-GC/MS overcomes this limitation.⁹⁴

Another method which has been utilized in determining SOA composition is electrospray ionization (ESI). High resolution electrospray ionization mass spectrometry (HR-ESI-MS) has been used to investigate limonene oxidation products from chamber studies.^{100,101}

In these experiments particles from the chamber are collected on substrates and extracted.

Because this technique requires that particle samples be extracted, only components which are soluble in the solvent are analyzed. In addition, the selection of solvent matters; the solvent may react with components of the particles, altering the chemical composition, unless careful control experiments identify the appropriate solvents. High resolution desorption electrospray ionization mass spectrometry (DESI-MS) may overcome some of the shortcomings of ESI-MS. This technique was recently used to study the aging of particles produced in a chamber.¹⁰² Using DESI-MS, samples spend much less time in the solvent, so there is less chance for reactions between the solvent and particle components, as well as reduced chance of breakdown of labile particle components. In addition, this analysis is carried out rapidly, using soft ionization, allowing for the quantitative identification of compounds such as conjugated nitrogen-containing particles,¹⁰² which are associated with light-absorbing brown carbon.¹⁰³

A shortcoming of mass spectrometry is that the particles are destroyed during analysis. Non-destructive methods for analyzing the chemical composition of SOA particles exist as well. In general, these methods involve offline analysis; in particular, Fourier transform infrared (FTIR) spectroscopy has become important for studying organic aerosol particles without the necessity of working under vacuum conditions, as is needed for synchrotron-based spectromicroscopy.¹⁰⁴ In particular, the Russell group¹⁰⁵ has applied transmission FTIR spectroscopy to microgram amounts of aerosol particle material on appropriately chosen filters, allowing for an exquisite speciation analysis and source apportionment of the organic and inorganic constituents within the organic particulate matter. The ability to distinguish between organic functional groups provides

increased chemical specificity versus the analysis of O/C ratios alone.¹⁰⁵ However, FTIR spectroscopy is not a single particle analysis technique, and therefore, single particle speciation is not possible. Also, due to the limited sensitivity of FTIR spectroscopy, particle samples are collected over long periods of time, restricting the time-resolution of speciation information. Further, particles must be dried as they are collected, in order to prevent interference from water absorption during analysis, and the drying process may impact the chemistry of the particles. FTIR analysis of particles may be correlated with NMR analysis, allowing for further determination of particle structure. For example, cross-polarization with magic-angle spinning (CPMAS) ¹³C NMR has been used to determine the distribution of organic functional groups within particles.¹⁰⁶ Unlike other forms of NMR analysis, which require liquid samples, CPMAS ¹³C NMR is non-destructive. However, this analysis requires a large amount of sample, greatly reducing temporal resolution during sample collection, as well as some sample manipulation, including separation of organic and inorganic components. For both FTIR and NMR spectroscopy, quantitative analysis may be difficult, and data interpretation is often not trivial.

Other methods applied to the analysis of organic aerosol particles, which are important for the work discussed here, include electron microscopy,^{107,108} as well as optical¹⁰⁹ and X-ray imaging.¹¹⁰ Scanning electron microscopy (SEM) and tunneling electron microscopy (TEM) produce images with high spatial resolution. These techniques are valuable for determining the elemental composition of single particles, especially of inorganic components, but are less useful in determining the oxidation states and hybridization of carbon, oxygen, and nitrogen. The use of SEM and TEM in combination with X-ray

techniques provides a more complete molecular understanding of organic species. Near edge X-ray absorption fine structure (NEXAFS) and scanning transmission X-ray microscope (STXM) spectrometry have proven useful for quantifying the organic functional groups present in aerosol particle samples. X-ray photoelectron spectroscopy (XPS) is useful in determining elemental composition and oxidation states on SOA particle surfaces, although care must be taken in comparing these results with those of other techniques, as XPS is a surface-specific technique.¹¹¹ The use of microscopic techniques is beneficial in that it allows for the determination of single particle chemical composition,⁵⁰ as well as morphology^{112,113} with good spatial resolution. However, obtaining statistically significant results from single particle analyses can be extremely time-consuming. In addition, since microscopic analysis is carried out offline, there is the possibility of sample contamination, and X-ray techniques require that analysis be carried out under vacuum conditions. Currently, it is difficult to determine the chemical composition of single particles smaller than approximately 200 nm under ambient conditions and in real time.¹¹⁴ As is discussed in the following section, coherent laser spectroscopies can overcome many of the limitations of the techniques used for the analysis of organic aerosol particles as they are applied directly to particles collected on filters and impactors without the need for vacuum conditions, particle extraction, destruction, or other sample manipulation.

VI. Vibrational Sum Frequency Generation (SFG) Spectroscopy of Organic Aerosol Particles. SFG¹¹⁵ is a powerful spectroscopic technique that has enabled much molecular insight into the heterogeneous atmospheric chemistry of laboratory model systems. Our group focused on oxidative C=C double bond cleavage chemistry involving flat surfaces

of oxides functionalized with atmospherically relevant molecules via silane chemistry,¹¹⁶⁻

¹²³ while other research groups have focused on the flat surfaces and interfaces of water.¹²⁴⁻¹³³ Excellent resources outlining the details of vibrational SFG exist,¹³⁴ and some of its applications in areas ranging from biophysics¹³⁵ to catalysis¹³⁶ and energy science^{137,138} to environmental chemistry¹³⁹ have been reported by us. Hallmarks of the method are an exquisite sensitivity to molecular structure within complex environments, a very high selectivity for environments where symmetry is broken, and heterodyne detection of weak vibrational responses, which allows for the analysis of nano-⁸⁰ to sub-femtogram¹⁴⁰ amounts of samples, including aerosol particles. While nonlinear optics had been applied to nano- and microparticles before,¹⁴¹⁻¹⁴⁶ the application of SFG to study atmospheric aerosol particles had not been presented prior to 2011, when our first reports on the subject appeared.^{80,147,148}

In the experiments (Figure 4),^{119-121,123,138} we use a broadband 120 fs infrared optical parametric amplifier running at a 1 kHz repetition rate. SFG spectra are obtained in triplicate with a hybrid scanning/broadband method pioneered by Walker and coworkers¹⁴⁹ by upconverting the IR light field using a visible pump beam from a regeneratively pumped Ti:S amplifier laser system filtered with a narrow band-pass filter yielding an 800 nm pump pulse with 1.57 nm bandwidth. To avoid optical damage, the incident pulse energies and foci are limited to 1 microjoule and 50 micrometers in diameter, respectively. We reference the SFG spectra to the SFG response from a gold substrate to account for the energy distribution in the IR field for each polarization combination, normalize to input power, and calibrate to the methyl CH stretches of a spectroscopic standard composed of polystyrene. Correct power dependencies of the SFG

responses are verified regularly. SFG experiments probing reference compounds, all of which have sufficiently high enough vapor pressures at room temperature,¹⁵⁰ at the surfaces of optical windows using a previously described¹⁵¹ custom-built chamber containing optical IR grade windows clamped upon a Teflon cell holding μL amounts of liquid sample with a void space to fill it with the equilibrium vapor pressure of the sample. Prior to use, all sample cell materials are rinsed and sonicated in methanol and Millipore water, followed by oven drying, and then plasma cleaning. SFG spectra of the optical windows after this procedure are void of CH stretching contributions.

VII. α -Pinene-Derived Aerosol Particles Prepared at the Harvard Environmental

Chamber. Figure 5A shows ssp-polarized SFG spectra of organic aerosol particles having a size of roughly 100 nm that were collected at the Harvard Environmental Chamber (HEC) in 2010 and of α -pinene vapor in contact with a fused silica window.⁸⁰

We recently described the details of this experiment, including the particle synthesis and characterization.^{80,147} The ssp polarization combination utilizes upconverter and infrared light that is plane-polarized parallel and perpendicular to the surface, respectively, and detects SFG signals that are polarized perpendicularly to the surface. For molecular adsorbates located at macroscopically flat substrates, such as the α -pinene reference compound adsorbed to a fused silica window (Figure 5A), the ssp polarization combination probes the components of vibrational modes that are oriented perpendicular to the surfaces. The ssp-polarized SFG spectrum of (+)- α -pinene exhibits the asymmetric and symmetric methyl CH stretches at 2960 cm^{-1} and 2880 cm^{-1} , respectively, as well as a methyl Fermi resonance at 2940 cm^{-1} , which dominates the spectral response. For comparison, the vibrational SFG spectra of cis-2-pentene, n-hexene, n-pentene,

cyclohexene, and cyclopentene vapor in contact with an α -alumina optical window, which we analyzed previously,¹⁵¹ show substantial signal intensity in the symmetric CH stretching region below 2900 cm^{-1} , which distinguishes them from the terpenes. While the SFG spectra of cyclohexene and cyclopentene clearly show vinylic CH stretches above 3000 cm^{-1} ,¹⁵¹ the olefinic CH stretch of (+)- α -pinene is not observed. Other polarization combinations, including those probing vibrational modes oriented perpendicular to the surface normal, do not reveal it either. This observation is attributed to the fact that the Raman polarizability and infrared transition moments of this single olefinic CH oscillator are weak. Figure 5A shows that the ssp-polarized SFG spectrum of synthetic SOA particles prepared at the HEC is shifted by about 20 cm^{-1} towards 2950 cm^{-1} , the tell-tale frequency of the Fermi resonance of the CH_3 symmetric stretch with a CH_3 bending overtone typical of CH_3 groups on long-chain aliphatic molecules.¹⁵²⁻¹⁵⁴ No new spectral features appear, which indicates that the particle material contains CH oscillators that produce SFG responses that are similar to those of α -pinene vapor in contact with a fused silica window.

Given that the two SFG spectra shown in Figure 5A are dominated by Fermi resonances involving the methyl CH stretches and/or their asymmetric stretches, isotope-editing the methyl groups of α -pinene should be very informative for the structural analysis of organic material derived from α -pinene. One important question is if the three methyl groups in α -pinene and the organic aerosol particle material derived from it add coherently, or if there is one type of methyl group that dominates the SFG response. Future work that is planned within our program will involve stepwise isotope editing. Such a synthesis approach will allow us to spectroscopically assign these very important

molecules, whose vibrational response in the CH stretching region has remained sparsely studied until now, and to produce important experimental spectroscopic benchmarks for their theoretical studies.

Until we have prepared the relevant isotope-edited compounds, we invoke mass spectrometric data by others, for instance from the Johnston group,^{76,77} which supports the idea that the four-membered ring of α -pinene remains closed upon ozone oxidation. Given the rigidity of this arrangement, strong vibrational coherences and coupling are expected for the CH stretching region, as is evident in the spectra shown in Figure 5A. We generally observe that, when compared to α -pinene, the methyl groups of aliphatic hydrocarbons, which possess much floppier carbon backbones than α -pinene, yield significantly less SFG signal intensity in the frequency region corresponding to the methyl asymmetric stretches and Fermi resonances.¹⁵¹ This then leads us to propose that the synthetic organic material prepared at the HEC consists of monomers, dimers, or possible oligomers having repeating units of four-membered rings with two methyl groups, similar to what is shown in Figure 3.

VIII. Aerosol Particles Formed in α -Pinene-Rich Air in Southern Finland.

A. Spectroscopic Analysis and Interpretation. Before taking the SFG spectra of the aerosol particles collected at the SMEAR II field sampling site, we applied contact mode atomic force microscopy (AFM) to the PM1 size fraction of aerosol particle material printed from one of the Teflon filters collected at the site onto a silicon wafer (Figure 5B). The AFM images were recorded using a Bioscope II Scanning Probe Microscope with a NanoScope® V controller (Digital Instruments) at a resolution of 512 x 512 lines and with V-shaped SNL-10 probes (Veeco) with a 0.12 N/m spring constant and a 16-28

kHz resonant frequency. The AFM images show irregularly shaped objects that have a height of up to 0.5 micrometers and diameters ranging from several hundred nm to around one micrometer that are randomly arranged in clusters and aggregates on the substrate. Organic molecules such as α -pinene and isoprene and their oxidation products have a size of about 1 nm and possess low symmetry, most often C_1 . When such molecules are located at the surfaces of irregularly shaped organic particles having sizes of several hundred nm, one can assume within a first-order approximation that the molecular orientation distributions are similar to those of macroscopically flat surfaces and thus invariant with location on the particle surface. For a pancake-shaped particle, the ssp-polarized SFG response is due to molecules located on top of the particle that have vibrational modes oriented perpendicular to the top of the particle surface (Figure 5C). Molecules located on the side of the particle that have vibrational modes oriented parallel to the particle surface will contribute to the ssp-polarized SFG response as well. Given that many more molecules are localized on the large flat portion of the particle than on the side, the ssp-polarized SFG responses are likely to originate mainly from the vibrational modes that are associated with those molecules that reside on the flat portion of the particle and that are oriented perpendicularly to that portion of the particle surface. While a systematic study of this situation is beyond the scope and relevance to this work, it is planned as part of our efforts in applying nonlinear optics to aerosol particles resting on flat impactor surfaces.

Fig. 6 shows a series of eleven ssp-polarized SFG spectra recorded from individual spots on eleven PM1 filters collected between 13 July 2010 and 25 July 2010, along with the ssp-polarized SFG spectra obtained for α -pinene- and isoprene-derived SOA material

synthesized at the HEC. The SFG spectra obtained from the field-collected particles are remarkably similar to that of the α -pinene model system, even though there are several samples that were collected on days during which isoprene concentrations exceeded α -pinene concentrations by a factor of up to 2 or 3 for multiple hours, as indicated by the vertical green dashed line. Signal contributions in the aromatic CH stretching region are generally weak if present at all, which is consistent with the ten-fold concentration excess of the terpenes over benzene and toluene, the typical markers for fossil burning activities, during this first half of the HUMPPA-COPEC campaign.

All the PM1 filters studied here are very uniform in their SFG response except for one, which was collected from 6AM to 6PM on 18 July 2010. Two out of five ssp-polarized SFG spectra obtained from five different spots on this filter, which are also shown in Fig. 6, are quite dissimilar from the other three. Their average exhibits the presence of one additional strong peak at 2915 cm^{-1} , which is not observed in the other spectra we recorded. This finding led us to investigate whether the SFG signal at 2915 cm^{-1} might be a signature of isoprene in the particles, as isoprene was quite abundant during the time of particle collection. However, the ssp-polarized SFG spectra of isoprene-derived synthetic aerosol particles prepared at the HEC are at variance with those obtained from the filter collected on 18 July 2010. We putatively attribute the new spectral feature to the possible presence of one or more of the compounds shown in Fig. 3, or to anthropogenic compounds such as benzene or toluene, which were both relatively high in concentration during the day preceding collection of the filter that exhibits the additional SFG spectra feature at 2915 cm^{-1} .

B. Nucleation Event. On the morning of 23 June 2010, the field site experienced an aerosol particle nucleation event, during which fresh, nearly terpene-free air from the Arctic entered the area. With the air being practically void of SOA particle precursors, the aerosol particle number density, measured by scanning mobility particle sizers (SMPS), dropped from more than 1000 particles per cm^3 to just ten or so particles per cm^3 , while the aerosol particle diameters dropped almost instantaneously from several hundred nm to just a few nm at 6AM. Terpene production by the forest continued, of course, and thus the aerosol particle population built up over the course of the day to about 1000 particles per cm^3 , with sizes ranging from 50 to 100 nm. Once printed from the PM1 collection filter onto the AFM substrate, the particles tend to clump up into those imaged by AFM (Fig. 5B). This finding may possibly indicate that the particles were already agglomerated on the filter.

While the spectroscopic analysis of the small number of nm-sized particles available for collection during the time of a nucleation event is a major challenge for most spectrochemical methods, it is possible through the strong coherent signals generated in the vibrational SFG spectroscopy of organic aerosol particles. Specifically, Fig. 6 shows the ssp-polarized SFG spectrum obtained from particles collected from the start of the nucleation event (6:00AM, as indicated by the horizontal dashed line) through 2:00PM of the same day. This spectrum was recorded in the same fashion as the other spectra shown in Fig. 6, namely by using two minutes per spectral acquisition, repeated seven times to increase the signal to noise ratio. While being the least intense SFG spectrum of the set, which is consistent with the low estimated mass of organic material on the filter ($<2 \mu\text{g}$), the spectral signature at 2945 cm^{-1} and the shoulder at 2880 cm^{-1} are clearly visible.

The sum of (+)- and (-)- α -pinene concentration at the beginning of the nucleation event at 6:00AM on 23 June 2010 was 28 ppt while it was 243 ppt for isoprene. This low ratio of α -pinene-to-isoprene concentrations persisted throughout the day. For instance, at 2PM, the stop-time for the filter whose ssp-polarized SFG spectrum is underlined by the green horizontal line, the ratio had increased to just 0.17. Finally, by 10:00PM of the same day, the ratio of α -pinene-to-isoprene concentrations had increased back to above 1.0. Yet, while isoprene concentrations far exceeded those of α -pinene during the daytime of 23 June 2010, isoprene-like SFG spectral signatures were not obtained from the PM1 size fraction of collected aerosol particles. Instead, the ssp-polarized SFG spectra are remarkably similar to those obtained throughout the majority of the two-week period studied. This strongly suggests that the SOA particles that were formed during the nucleation event are composed, at least as probed by vibrational SFG spectroscopy, of derivatives of α -pinene and not of isoprene, which is consistent with the fact that the oxidative chemistry in boreal forest regions is dominated by O_3 as opposed to OH radicals. We conclude from the data presented in Fig. 6 that in as far as SFG probes the chemical composition of aerosol particles, the α -pinene-derived organic material synthesized at the HEC is a reasonable model for organic aerosol particles formed during the summertime in Southern Finland that represents well around 90% of organic material collected on the filters examined here by SFG.

C. Molecular Chirality and the Aerosol Particle and Gas Phases. In 2009, we published an article discussing the possible role of atmospheric heterogeneous stereochemistry in aerosol chemistry and physics.¹⁵⁵ While chirality effects in terpene biosynthesis¹⁵⁶ as well as in reverse micelles, which may be invoked as aerosol particle

models,^{157,158} have been studied for quite some time now,¹⁵⁹ the topic of chirality in atmospheric chemistry is now just emerging,^{160,161} with a few groups, including ours,^{147,148,155} studying specifically chirality in organic aerosol particles.¹⁶²⁻¹⁶⁴ Using the psp-polarization combination,¹⁶⁵ which accesses several elements of the nonlinear susceptibility tensor, including the χ_{xyz} tensor element that is uniquely non-zero for all chiral species, it is possible to obtain non-zero chiral vibrational SFG signatures from aerosol particles collected during the summer in Southern Finland in the PM1 size fraction (Fig. 7A). Specifically, we find a single vibrational resonance at 2960-2950 cm^{-1} , which agrees well with the one we obtained from synthetic SOA particle samples prepared at the HEC from varying ratios of (+)- and (-)- α -pinene using a related polarization combination.¹⁴⁷ Aerosol particles collected in March of 2011, the early spring following the HUMPPA-COPEC-2010 field intensive, show minor to negligible chiral SFG signals, even though the ssp-polarized SFG spectrum, which samples mainly achiral contributions, shows the presence of α -pinene-derived organic material (Fig. 7B). Future experiments require the determination of the enantiomeric excess (EE) of (+)- over (-)- α -pinene in the gas phase to assess whether the absence of a chiral SFG signal in the aerosol particles collected in March 2011 indicates if the particles on the filter samples do not contain chiral species or if they contain racemates.

Prior analysis of events occurring during the HUMPPA-COPEC field campaign identified two days during which the field measurement site was downwind from operating sawmills,³ namely 18 July 2010 and 6 August 2010. Due to the fact that the boundary layer becomes shallow and emissions from the freshly sawn wood are advected most effectively to the site late at night, the (+)- α -pinene EE in the air at the field

measurement site was around 50% during the early morning hours, as indicated by the white asterisks in Fig. 7A. The top psp-polarized SFG signal shown in Fig. 7A was obtained from particles that were collected over an 8-hour period during the 6 August 2010 saw mill event. We interpret the strong psp-polarized SFG response to be a signature of the large excess of (+)- α -pinene in the air that apparently had enough time to be incorporated into the collected aerosol particles. The middle spectrum was obtained from particles collected over a 24 hour period while there was no saw mill activity and also relatively low EE of (+)- α -pinene in the air, and it exhibits minor psp-polarized SFG intensity. Finally, the bottom spectrum was obtained from particles collected during a 12 hour period which included pronounced saw mill activity, albeit on its tail end, and also pronounced EE of (+)- α -pinene in the air during times preceding the saw mill event, and its psp-polarized SFG intensity is between that of the two spectra above it. In summary, Fig. 7 shows that EEs of (+)- α -pinene in air below 20% or so lead to minor psp-polarized SFG responses unless events associated with much higher EE values precede particle collection by several hours. When particle collection coincides with high EE values, then the psp response is appreciable as well, which is consistent with our previously published model study.¹⁴⁷ If the psp-polarized SFG spectra are dominated by the vibrational responses of chiral molecules, then it should be possible to connect – in time – the enantiomeric composition of the particles with the enantiomeric composition of the gas phase. One could therefore use chirality as a marker, or label, for determining the rates of aerosol formation from gas phase constituents. Use of such a “chiral marker” could then help answer whether aerosol particles present in air at a certain hour on a certain day were formed from VOCs that were present in air three, six, 12, or 24 hours earlier. The

fact that the (+)- α -pinene EE is anticorrelated with the diurnal cycle makes the concept of a “chiral marker” a real possibility for understanding aerosol particle formation.

IX. Aerosol Particles Collected from Air Rich in Isoprene (Amazonia). To contrast atmospheric aerosol chemistry and physics in the boreal forest with that of tropical forests, we present in this section results obtained by vibrational SFG from aerosol particles collected in the central Amazon Basin. Unlike in the previous section, the Amazonian field campaign sampled organic aerosol particles using MOUDIs, so our discussion will center on the spectral analysis of highly size-resolved aerosol particles. As the chemical reactions for the formation of organic aerosol particles is likely to be dominated by isoprene oxidation by OH radicals (Table I), we begin by discussing the ssp-polarized SFG spectra obtained from isoprene-derived particles synthesized in 2010 at the Harvard Environmental Chamber (HEC) and of isoprene vapor in contact with a fused silica window (Fig. 8A).⁸⁰ Unlike in the case of α -pinene and its oxidation products (Fig. 5), the organic material prepared from isoprene oxidation by OH radicals at the HEC (here, ppb levels of OH radicals are used as an oxidant, as described in our published work)⁸⁰ is spectrally quite dissimilar from the isoprene precursor: the vinylic CH stretches above 3000 cm^{-1} are clearly observable for isoprene, which also shows asymmetric and symmetric CH stretches at 2950 cm^{-1} and 2850 cm^{-1} , respectively, as well as a strong vibrational resonance at 2900 cm^{-1} . The absence of vinylic CH stretches in the SFG spectrum of the isoprene-derived organic material from the HEC is consistent with C=C double bond oxidation. In fact, the appearance of asymmetric and symmetric methyl and symmetric methylene stretches at 2950 cm^{-1} , 2880 , and 2850 cm^{-1} , respectively, and

the disappearance of the vinylic CH stretch of isoprene, suggest the formation of aliphatic compounds containing methyl groups upon SOA formation.

Fig. 8B and 8C show the ssp-polarized SFG spectra of the coarse and fine modes, respectively, of organic aerosol particles collected on nucleopore impactor substrates using a MOUDI operating from 9 April 2008 to 17 April 2008 at the site of the AMAZE-08 campaign described in section II. Fig. 8B shows that the particle material in the coarse mode, which samples sizes larger than one micron, exhibits many spectral features that are different with each new sample spot on the same filter. For instance, the top three spectra displayed in Fig. 8B are obtained from three different spots on MOUDI stage 3, and none resemble one another. The chemical complexity of these particles in the coarse mode that is reflected by their spectral variability is likely due to the presence of primary biological material such as pollen or plant debris in these particles.¹⁶⁶ The three SFG spectra of the particles collected on three spots of the filter holding the next smaller size fraction (1.8 μm) are much more similar to one another but weaker in intensity.

In contrast to what we observe in the coarse mode, the ssp-polarized SFG spectra obtained from submicron sized particles (Fig. 8C) are roughly invariant with size: for particles with aerodynamic diameter 50% cutoffs of 1.0 μm , 560 nm, and 330 nm, there is little variability in the SFG spectra, at least in the CH stretching region. The isoprene-derived organic material prepared at the HEC and the isoprene precursor exhibit no peak at 2900 cm^{-1} , which is prominent in the fine mode of the field-collected aerosol particle samples. As reported by Wenberg and coworkers in 2009,¹⁶⁷ isoprene can undergo photooxidation in the gas phase to produce epoxides. Formation of methyltetrols has been reported as well by Claeys and coworkers,^{24,168} and these compounds could be the origin

of the spectral features observed in the SFG spectra shown in Fig. 8C. However, until we have prepared the proper reference compounds for analysis by SFG spectroscopy, it is not possible for us to confirm the presence of epoxides, tetrols, or related compounds in the isoprene-derived organic material synthesized at the HEC or collected in the central Amazon Basin.

To assess whether the SFG signal intensities depend on the bulk optical properties of the sample material on the various MOUDI stages, we recorded their reflectivity spectra. This was carried out because of the low transmittivity of the MOUDI stage substrates, which are made of Teflon. Given that the high dilution of just a few μg of aerosol particle material over the entire one-inch area of each MOUDI stage make linear optical imaging and reflectivity measurements challenging, we show in Fig. 8C the optical images and reflectivities of a set of MOUDI stages that were collected from 1 May to 10 May 2008 while the rotating motor gearbox was disengaged. This situation fortuitously resulted in enough material under each of the microorifices, as shown in the insets of the bottom five optical images, that reflectivity data could be readily collected using our spectrophotometer while simultaneously providing background reflectivities from uncoated areas, as shown in the gray spectra in Fig. 8C. In general, we find that the aerosol particle material on the MOUDI stages appears round or elliptical except for the stage selecting the largest sizes, which is likely due to primary emissions from plants, such as pollen. The reflectivity spectra show that the samples become more reflective at wavelengths shorter than 600 nm with smaller the particle size except for the very last stage (0.093 μm), which is likely due to somewhat elevated black carbon content expected from the biomass burning season that starts around that time. At the SFG signal

wavelength of ~640 nm, the reflectivities do not appear to change significantly with aerodynamic size range for those stages of which we took SFG spectra, which suggests that optical absorption of the SFG signal at this wavelength contributes negligibly to the SFG signal intensities of the spectra discussed here.

In the experiments, the optical images were obtained using ultra-long working distance epiplan-neofluar 10x and 50x objectives (80% and 85% transmission at 400 nm, Zeiss part # 4220409902000000 and 4224729900000000, respectively, the latter of which having a 9.1 mm working distance) with numerical apertures of 0.2 and 0.55, respectively, resulting in a maximum resolution of 1.2 μm and 0.4 μm , respectively, calculated for a nominal wavelength of 400 nm. Using a Zeiss tube lens (part # 452149-0000) having 95% transmission at 400 nm housed inside a Zeiss binocular phototube (part #4255209030000000) and an Axioscope focusing gear box (part # 4300369000000000), the image is detected on a thermoelectrically cooled CCD detector (Princeton Instruments PIXIS 1024, 60% quantum efficiency at 400 nm) mounted onto the upper body part of a Zeiss Axioscope (part #4237309030000000) located on an Axisoscope stand column (part # 4510179000000000). The external, normal incident illumination occurs via a Zeiss LED illuminator (part # 4239049902000000), and optical reflectivities at normal incidence of illumination and detection were obtained using an Ocean Optics spectrophotometer coupled to the Zeiss binocular phototube using the appropriate fiberoptic.

Fig. 8C shows that whatever the chemical composition of the submicron SOA particles collected in the central Amazon Basin is, the size-invariance of their SFG responses suggests that the growth of these particles in the Aitken and accumulation modes is not

due to chemical reactions on the surface of and within the particle phase, but rather to condensation of terpene derivatives onto the particles. This process appears to occur such that whatever changes occur in the chemical composition of the particles of which we collect vibrational SFG spectra, changes in these spectra are minor. This interpretation suggests that the chemical composition of the SOA particles studied here is relatively uniform, at least as probed our coherent spectroscopy, throughout the 100 nm to 3000 nm size range. The O/C ratios of 0.3 to 0.5 that are typical for these particles (Table I)⁸⁰ support this interpretation.

X. Aerosol Particles from Anthropogenically Influenced Air (Blodgett Forest). We conclude our discussion by contrasting the SFG spectra of aerosol particles collected in Southern Finland and the central Amazon Basin with those obtained from particles collected in Blodgett Forest, CA. The aerosol particles were collected from 1-4 July 2009, 4-8 July 2009, 11-14 July 2009, and 25-28 July 2009 with a 2.5 μm cutoff. Back-trajectories for the period of time from 1-4 July indicate that the air masses arriving at the site during this time were predominantly from the west and southwest. These air masses passed over the Sacramento Valley before arriving at the sampling site, so there is large potential for anthropogenic influence in this particle sample. Back-trajectories for the sample collected from 25-28 July indicate that the air masses present during the formation of these particles were more variable in origin, sometimes originating from the west/southwest and at other times originating from the less populous north.

The ssp-polarized SFG response in the CH stretching region of these particles depends largely on the origin of the air present during their formation. Signal contributions above 3000 cm^{-1} , as seen in the top two spectra of Fig. 9, indicate the presence of aromatic

material in the particles, which is attributable to anthropogenic emissions such as those produced from fossil fuel burning that were entrained in the air as it moved through the Sacramento Valley towards the sampling location.^{169,170} The large non-resonant contributions in the spectra are indicative of highly polarizable materials such as carbon.^{137,171,172}

One of the spots on the filter collected during July 4-8 2009 yielded a spectrum that is comparable to that of α -pinene SOA. We note that Bouvier-Brown et al. reported that β -pinene is the dominant monoterpene in Blodgett Forest.³³ In our future work, we will characterize β -pinene-derived SOA particle material, which will be synthesized in the Harvard Environmental Chamber. The expectation is that of the four-membered ring with the two methyl groups, which both α - and β -pinene possess, dominate the coherent vibrational SFG response of SOA particles formed from them, then it may not be straight-forward to distinguish α - from β -pinene-derived SOA material by SFG.

The SFG spectrum resembling that of the α -pinene SOA reference material synthesized at the HEC is comparable in terms of peak positions to those obtained from aerosol particles collected during 11-14 and 25-28 July 2009 with the exception of the spectrum shown at the bottom of Fig. 9. As mentioned above, anthropogenic influences were variable during these days, and the aromatic contributions at 3200 cm^{-1} that can be seen in the bottom spectrum of Fig. 9 may be associated with aerosol particles containing emissions from fossil fuel combustion. We conclude from the spectra shown in Fig.9 that anthropogenic influences at the Blodgett forest sampling sites are readily identified by SFG in the sub- $2.5\text{ }\mu\text{m}$ size fraction of aerosol particles collected there, in fact, much more so than in Southern Finland, at least during the time periods studied here.

XI. Conclusion.

In conclusion, we have analyzed natural aerosol particles from three different forest environments using vibrational sum frequency generation. The experiments were carried out directly on filter and impactor substrates, without the need for sample pre-concentration, manipulation, or destruction. As part of this Feature Article, we have shed light on the important first steps leading to SOA particle nucleation and growth from α -pinene by showing that, at least as viewed by vibrational coherent spectroscopy, the chemical composition is close to size-invariant over the size range studied here. We also introduced the concept of molecular chirality as a chemical marker that could be useful for quantifying how chemical constituents in the SOA gas phase and the SOA particle phase are related in time. In addition, we have shown how micrograms of SOA particle material on a one- or two-inch collection filter are readily analyzed by vibrational sum frequency spectroscopy in a non-destructive fashion that does not require pumping on the sample or cooling it. Finally, we have described how the combination of multiple disciplines, such as aerosol science, advanced vibrational spectroscopy, meteorology, and chemistry can be highly informative when studying particles collected during atmospheric chemistry field campaigns, such as those carried out during AMAZE-08, HUMPPA-COPEC-2010, or BEARPEX, and when they are compared to results from synthetic model systems such as the Harvard Environmental Chamber. Future work will capitalize on these advances and include the study of synthetic putative SOA particle components such as those exhibited in Fig. 3 in order to pursue detailed spectroscopic assignments by vibrational SFG, prepare deuterium-labeled SOA particle precursors to fast-forward, in terms of mechanistic studies, through the SOA particle formation

process, and to further understand the role of molecular chirality in atmospheric chemistry.

XII. Acknowledgments. We thank Stephanie R. Walter and Joseph G. Holland for recording the tapping mode AFM images. We gratefully acknowledge data provided by Ron Cohen of the University of California, Berkeley. CJE gratefully acknowledges an NSF Graduate Research Fellowship. ALC acknowledges a DOE Office of Science Graduate Fellowship. JW acknowledges support from the European Community Research (ERC) Infrastructure Action Contract N° RII3-CT-2006-026140 Infrastructure for Measurements, ERC Grant ATMNUCLE (project No 227463), Academy of Finland Center of Excellence program (project No 1118615), the European Integrated Project on Aerosol Cloud Climate and Air Quality Interactions EUCAARI (project No 036833-2), the EUSAAR TNA (project No 400586), and the IMECC TA (project No 4006261). PA acknowledges the support of FAPESP and CNPq for grants that funded part of this work. STM thanks the Office of Science (BES), U.S. Department of Energy, for support under grant No. DE- FG02-08ER64529 and gratefully acknowledges support from the US National Science Foundation under grant # NSF ATM-0723582. LMR acknowledges support from the National Science Foundation Atmospheric Geospace Science division under grant # NSF ATM-0904203. FMG thanks the NSF Atmospheric and Geospace Science division for support under grant # NSF ATM-0533436. We acknowledge helpful discussions with Mark Peterson. The authors also thank Spectra Physics, a Division of Newport Corporation, for equipment loans and donations as well as superb technical support. FMG gratefully acknowledges support from an Irving M. Klotz professorship in physical chemistry.

References

- (1) IPCC, 2007: *Summary for Policymakers. In: Climate Change 2007: The Physical Science Basis. Contribution of Working Group I to the Fourth Assessment Report of the Intergovernmental Panel on Climate Change* Cambridge University Press: Cambridge, UK, 2007.
- (2) IPCC *Climate Change 2001: The Scientific Basis. Contribution of Working Group I to the Third Assessment Report of the Intergovernmental Panel on Climate Change*; Cambridge University Press: New York, NY, USA, 2001.
- (3) Williams, J.; Crowley, J. N.; Fischer, H.; Harder, H.; Martinez, M.; Petaja, T.; Rinne, J.; Back, J. B.; Boy, M.; Dal Maso, M.; Aalto, J.; Aaltonen, H.; Hakala, J.; Kajos, M.; Keronen, P.; Rantala, P.; Levula, J.; Pohja, T.; Hakola, H.; Paatero, J.; Vesala, T.; Herrmann, F.; Auld, J.; Mesarchaki, E.; Song, W.; Yassaa, N.; Noelscher, A.; Johnson, A.; Custer, T.; Sinha, V.; Thieser, J.; Pouvesle, N.; Taraborrelli, D.; Tang, M. J.; Bozem, H.; Hosaynali-Beygi, Z.; Axinte, R.; Oswald, R.; Novelli, A.; Kubistin, D.; Korbinian, H.; Javed, U.; Trawny, K.; Breitenberger, C.; Hidalgo, P. J.; Ebben, C. J.; Geiger, F. M.; Corrigan, A. L.; Russell, L. M.; Ouwensloot, H.; Vila-Guerau de Arellano, J.; Ganzeveld, L.; Vogel, A.; Beck, M.; Bayerle, A.; Kampf, C. J.; Hoffmann, T.; Valverde, J.; Gonzalez, D.; Riekkola, M.-L.; Kulmala, M.; Lelieveld, J. *ACP* **2011**, *11*, 10599.
- (4) Rinne, H. J. I.; Guenther, A. B.; Greenberg, J. P.; Harley, P. C. *Atmos. Env.* **2002**, *36*, 2421.
- (5) Lluisa, J.; Penuelas, J. *Am. J. Botany* **2000**, *87*, 133.
- (6) Penuelas, J.; Lluisa, J. *Biologia Plantarum* **2001**, *44*, 481.
- (7) *Climate Change 2007: The Physical Science Basis*; Cambridge University Press: Cambridge, UK, 2007.
- (8) Hallquist, M.; Wenger, J. C.; Baltensperger, U.; Rudich, Y.; Simpson, D.; Claeys, M.; Dommen, J.; Donahue, N. M.; George, C.; Goldstein, A. H.; Hamilton, J. F.; Herrmann, H.; Hoffmann, T.; Iinuma, Y.; Jang, M.; Jenkin, M. E.; Jimenez, J. L.; Kiendler-Scharr, A.; Maenhaut, W.; McFiggans, G.; Mentel, T. F.; Monod, A.; Prevot, A. S. H.; Seinfeld, J. H.; Surratt, J. D.; Szmigielski, R.; Wildt, J. *ACP* **2009**, *9*, 5155.
- (9) Goldstein, A. H.; Galbally, I. E. *Env. Sci. Technol.* **2007**, *41*, 1515.
- (10) Kanakidou, M.; Seinfeld, J. H.; Pandis, S. N.; Barnes, I.; Dentener, F. J.; Facchini, M. C.; Van Dingenen, R.; Ervens, B.; Nenes, A.; Nielsen, C. J.; Swietlicki, E.; Putaud, J. P.; Balkanski, Y.; Fuzzi, S.; Horth, J.; Moortgat, G. K.; Winterhalter, R.; Myhre, C. E. L.; Tsigaridis, K.; Vignati, E.; Stephanou, E. G.; Wilson, J. *ACP* **2005**, *5*, 1053.
- (11) Galbally, I. E.; Lawson, S. J.; Weeks, I. A.; Bentley, S. T.; Gillett, R. W.; Meyer, M.; Goldstein, A. H. *Environ. Chem.* **2007**, *4*, 178.
- (12) Riipinen, I.; Pierce, J. R.; Yli-Juuti, T.; Nieminen, T.; Hakkinen, S.; Ehn, M.; Junninen, H.; Lehtipalo, K.; Petaja, T.; Slowik, J.; Chang, R.; Shantz, N. C.; Abbatt, J.; Leaitch, W. R.; Kerminen, V. M.; Worsnop, D. R.; Pandis, S. N.; Donahue, N. M.; Kulmala, M. *Atmospheric Chemistry and Physics* **2011**, *11*, 3865.
- (13) Donahue, N. M.; Tischuk, J. E.; Marquis, B. J.; Hartz, K. E. H. *Physical Chemistry Chemical Physics* **2007**, *9*, 2991.

- (14) Inuma, Y.; Boge, O.; Keywood, M.; Gnauk, T.; Herrmann, H. *Environmental Science & Technology* **2009**, *43*, 280.
- (15) Pun, B. K.; Seigneur, C.; Lohman, K. *Environmental Science & Technology* **2006**, *40*, 4722.
- (16) Song, C.; Na, K.; Warren, B.; Malloy, Q.; Cocker, D. R. *Environmental Science & Technology* **2007**, *41*, 6990.
- (17) Ziemann, P. J. *J. Phys. Chem. A* **2003**, *107*, 2048.
- (18) Fenske, J. D.; Kuwata, K. T.; Houk, K. N.; Paulson, S. E. *J. Phys. Chem. A* **2000**, *104*, 7246.
- (19) Atkinson, R.; Arey, J. *Acc. Chem. Res.* **1998**, *31*, 574.
- (20) Kalberer, M.; Paulsen, D.; Sax, M.; Steinbacher, M.; Dommen, J.; Prevot, A. S. H.; Fisseha, R.; Weingartner, E.; Frankevich, V.; Zenobi, R.; Baltensperger, U. *Science* **2004**, *303*, 1659.
- (21) Mueller, L.; Reinnig, M.-C.; Warnke, J.; Hoffmann, T. *ACP* **2008**, *8*, 1423.
- (22) Gao, Y.; Hall IV, W. A.; Johnston, M. V. *Env. Sci. Technol. in press* **2010**.
- (23) Yasmeen, F.; Vermeylen, R.; Szmigielski, R.; Inuma, Y.; Boege, O.; Herrmann, H.; Maenhaut, W.; Claeys, M. *ACP* **2010**, *10*, 10865.
- (24) Claeys, M.; Inuma, Y.; Szmigielski, R.; Surratt, J. D.; Blockhuys, F.; Van Alsenoy, C.; Boege, O.; Sierau, B.; Gomez-Gonzalez, Y.; Vermeylen, R.; Van der Veken, P.; Shahgholi, M.; Chan, A. W. H.; Herrmann, H.; Seinfeld, J. H.; Maenhaut, W. *ES&T* **2009**, *43*, 6976.
- (25) Paulot, F.; Crounse, J. D.; Kjaergaard, H. G.; Kurten, A.; St Clair, J. M.; Seinfeld, J. H.; Wennberg, P. O. *Science* **2009**, *325*, 730.
- (26) Crounse, J. D.; Paulot, F.; Kjaergaard, H. G.; Wennberg, P. O. *PCCP* **2011**, *13*, 13607.
- (27) Tolocka, M. P.; Jang, M.; Ginter, J. M.; Xoc, F. J.; Kamens, R. M.; Johnston, M. V. *ES&T* **2004**, *38*, 1428.
- (28) Kroll, J. H.; Seinfeld, J. H. *Atmos. Env.* **2008**, *42*, 3593.
- (29) Docherty, K. S.; Wu, W.; Kim, Y. B.; Ziemann, P. J. *ES&T* **2005**, *39*, 4049.
- (30) Heaton, K. J.; Slighter, R. L.; Hatcher, P. G.; Hall IV, W. A.; Johnston, M. V. *ES&T* **2009**, *43*, 7797.
- (31) Chen, Q.; Liu, Y.; Donahue, N. M.; Shilling, J. E.; Martin, S. T. *Env. Sci. Technol.* **2011**, *45*, 4763.
- (32) Martin, S. T.; Andreae, M. O.; Althausen, D.; Artaxo, P.; Baars, H.; Borrmann, S.; Chen, Q.; Farmer, D. K.; Guenther, A.; Gunthe, S. S.; Jimenez, J. L.; Karl, T.; Longo, K.; Manzi, A.; Pauliquevis, T.; Petters, M. D.; Prenni, A. J.; Poschl, U.; Rizzo, L. V.; Schneider, J.; Smith, J. N.; Swietlicki, E.; Tota, J.; Wang, J.; Wiedensohler, A.; Zorn, S. R. *Atmos. Chem. Phys.* **2010**, *10*, 11415.
- (33) Bouvier-Brown, N. C.; Goldstein, A. H.; Gilman, J. B.; Kuster, W. C.; de Gouw, J. A. *Atmospheric Chemistry and Physics* **2009**, *9*, 5505.
- (34) Andreae, M. O.; Artaxo, P.; Brandao, C.; Carswell, F. E.; Ciccioli, P.; da Costa, A. L.; Culf, A. D.; Esteves, J. L.; Gash, J. H. C.; Grace, J.; Kabat, P.; Leslieveld, J.; Malhi, Y.; Manzi, A.; Meixner, F. X.; Nobre, A. D.; Nobre, C.; Ruivo, M. D. L. P.;

Silva-Dias, M. A.; Stefani, P.; Valentini, R.; von Jouanne, J.; Waterloo, M. J. *J. Geophys. Res.* **2002**, *107*, 8066.

(35) Guenther, A.; Hewitt, C. N.; Erickson, D.; Fall, R.; Geron, C.; Graedel, T.; Harley, P.; Klinger, L.; Lerdau, M.; McKay, W. A.; Pierce, T.; Scholes, B.; Steinbrecher, R.; Tallamraju, R.; Taylor, J.; Zimmerman, P. *Journal of Geophysical Research-Atmospheres* **1995**, *100*, 8873.

(36) Kesselmeier, J.; Guenther, A.; Hoffmann, T.; Warnke, J. In *Amazonia and Global Change*; Keller, M., Gash, J., Silva Dias, P., Eds. 2009, p in press.

(37) Vrekoussis, M.; Wittrock, F.; Richter, A.; Burrows, J. P. *Atmospheric Chemistry & Physics* **2009**, *13*, 4485.

(38) Lelieveld, J.; Butler, T. M.; Crowley, J. N.; Dillon, T. J.; Fischer, H.; Ganzeveld, L.; Harder, H.; Lawrence, M. G.; Martinez, M.; Taraborrelli, D.; Williams, J. *Nature* **2008**, *452*, 737.

(39) Artaxo, P.; Maenhaut, W.; Storms, H.; Vangrieken, R. *Journal of Geophysical Research-Atmospheres* **1990**, *95*, 16971.

(40) Andreae, M. O. *Science* **2007**, *315*, 50.

(41) Andreae, M. O.; Artaxo, P.; Brandao, C.; Carswell, F. E.; Ciccioli, P.; da Costa, A. L.; Culf, A. D.; Esteves, J. L.; Gash, J. H. C.; Grace, J.; Kabat, P.; Lelieveld, J.; Malhi, Y.; Manzi, A. O.; Meixner, F. X.; Nobre, A. D.; Nobre, C.; Ruivo, M.; Silva-Dias, M. A.; Stefani, P.; Valentini, R.; von Jouanne, J.; Waterloo, M. J. *Journal of Geophysical Research-Atmospheres* **2002**, *107*, 8066.

(42) Claeys, M.; Graham, B.; Vas, G.; Wang, W.; Vermeylen, R.; Pashynska, V.; Cafmeyer, J.; Guyon, P.; Andreae, M. O.; Artaxo, P.; Maenhaut, W. *Science* **2004**, *303*, 1173.

(43) Gerab, F.; Artaxo, P.; Gillett, R.; Ayers, G. *Nuc. Instr. Meth. Phys. Res. B.* **1998**, *137*, 955.

(44) Martin, S. T.; Andreae, M. O.; Artaxo, P.; Baumgardner, D.; Chen, Q.; Goldstein, A. H.; Guenther, A.; Heald, C. L.; Mayol-Bracero, O. L.; McMurry, P. H.; Pauliquevis, T.; Pöschl, U.; Prather, K. A.; Roberts, G. C.; Saleska, S. R.; Silva-Dias, M. A.; Spracklen, D. V.; Swietlicki, E.; Trebs, I. *Rev. Geophys.* **2010**, *48*, RG2002.

(45) Goldstein, A. H.; Hultman, N. E.; Fracheboud, J. M.; Bauer, M. R.; Panek, J. A.; Xu, M.; Qi, Y.; Guenther, A. B.; Baugh, W. *Agric. For. Meteorol.* **2000**, *101*, 113.

(46) Marple, V. A.; Rubow, K. L.; Behm, S. M. *Aerosol Sci. Technol.* **1991**, *14*, 434.

(47) In *IPCC 2007 Assessment Report 4*; Pachauri, R. K., Reisinger, A., Eds.; IPCC: Geneva, Switzerland, 2007, p 104.

(48) Dal Maso, M.; Kulmala, M.; Riipinen, I.; Wagner, R.; Hussein, T.; Aalto, P. P.; Lehtinen, K. E. J. *Boreal Environ. Res.* **2005**, *10*, 323.

(49) Engelhart, G. J.; Hildebrandt, L.; Kostenidou, E.; Mihalopoulos, N.; Donahue, N. M.; Pandis, S. N. *Atmospheric Chemistry and Physics* **2011**, *11*, 911.

(50) McMurry, P. H. *Atmos. Environ.* **2000**, *34*, 1959.

(51) Hirsikko, A.; Bergman, T.; Laakso, L.; Dal Maso, M.; Riipinen, I.; Horrak, U.; Kulmala, M. *Atmospheric Chemistry and Physics* **2007**, *7*, 201.

(52) Tammet, H. *Atmospheric Research* **2006**, *82*, 523.

(53) Mirme, A.; Tamm, E.; Mordas, G.; Vana, M.; Uin, J.; Mirme, S.; Bernotas, T.; Laakso, L.; Hirsikko, A.; Kulmala, M. *Boreal Environ. Res.* **2007**, *12*, 247.

(54) Manninen, H. E.; Nieminen, T.; Asmi, E.; Gagne, S.; Hakkinen, S.; Lehtipalo, K.; Aalto, P.; Vana, M.; Mirme, A.; Mirme, S.; Horrak, U.; Plass-Dulmer, C.; Stange, G.; Kiss, G.; Hoffer, A.; Toeroe, N.; Moerman, M.; Henzing, B.; de Leeuw, G.; Brinkenberg, M.; Kouvarakis, G. N.; Bougiatioti, A.; Mihalopoulos, N.; O'Dowd, C.; Ceburnis, D.; Arneth, A.; Svenningsson, B.; Swietlicki, E.; Tarozzi, L.; Decesari, S.; Facchini, M. C.; Birmili, W.; Sonntag, A.; Wiedensohler, A.; Boulon, J.; Sellegri, K.; Laj, P.; Gysel, M.; Bukowiecki, N.; Weingartner, E.; Wehrle, G.; Laaksonen, A.; Hamed, A.; Joutsensaari, J.; Petaja, T.; Kerminen, V. M.; Kulmala, M. *Atmospheric Chemistry and Physics* **2010**, *10*, 7907.

(55) Manninen, H. E.; Petaja, T.; Asmi, E.; Riipinen, I.; Nieminen, T.; Mikkila, J.; Horrak, U.; Mirme, A.; Mirme, S.; Laakso, L.; Kerminen, V.-M.; Kulmala, M. *Boreal Environ. Res.* **2009**, *14*, 591.

(56) Kulmala, M.; Riipinen, I.; Sipila, M.; Manninen, H. E.; Petaja, T.; Junninen, H.; Dal Maso, M.; Mordas, G.; Mirme, A.; Vana, M.; Hirsikko, A.; Laakso, L.; Harrison, R. M.; Hanson, I.; Leung, C.; Lehtinen, K. E. J.; Kerminen, V.-M. *Science* **2007**, *318*, 89.

(57) Mirme, S.; Mirme, A.; Minikin, A.; Petzold, A.; Horrak, U.; Kerminen, V. M.; Kulmala, M. *Atmospheric Chemistry and Physics* **2010**, *10*, 437.

(58) Ehn, M.; Junninen, H.; Schobesberger, S.; Manninen, H. E.; Franchin, A.; Sipila, M.; Petaja, T.; Kerminen, V. M.; Tammet, H.; Mirme, A.; Mirme, S.; Horrak, U.; Kulmala, M.; Worsnop, D. R. *Aerosol Sci. Technol.* **2011**, *45*, 522.

(59) Petters, M. D.; Kreidenweis, S. M. *Atmospheric Chemistry and Physics* **2007**, *7*, 1961.

(60) Wex, H.; Stratmann, F.; Topping, D.; McFiggans, G. *Journal of the Atmospheric Sciences* **2008**, *65*, 4004.

(61) Hatch, C. D.; Gierlus, K. M.; Zahardis, J.; Schuttlefield, J.; Grassian, V. H. *Environmental Chemistry* **2009**, *6*, 380.

(62) Prenni, A. J.; Petters, M. D.; Kreidenweis, S. M.; DeMott, P. J.; Ziemann, P. J. *Journal of Geophysical Research-Atmospheres* **2007**, *112*.

(63) Pringle, K. J.; Tost, H.; Pozzer, A.; Poschl, U.; Lelieveld, J. *Atmospheric Chemistry and Physics* **2010**, *10*, 5241.

(64) Shinzuka, Y.; Clarke, A. D.; DeCarlo, P. F.; Jimenez, J. L.; Dunlea, E. J.; Roberts, G. C.; Tomlinson, J. M.; Collins, D. R.; Howell, S. G.; Kapustin, V. N.; McNaughton, C. S.; Zhou, J. *Atmospheric Chemistry and Physics* **2009**, *9*, 6727.

(65) Chang, R. Y. W.; Slowik, J. G.; Shantz, N. C.; Vlasenko, A.; Liggio, J.; Sjostedt, S. J.; Leaitch, W. R.; Abbatt, J. P. D. *Atmospheric Chemistry and Physics* **2010**, *10*, 5047.

(66) Good, N.; Coe, H.; McFiggans, G. *Atmos. Meas. Tech.* **2010**, *3*, 1241.

(67) Duplissy, J.; Gysel, M.; Alfarra, M. R.; Dommen, J.; Metzger, A.; Prevot, A. S. H.; Weingartner, E.; Laaksonen, A.; Raatikainen, T.; Good, N.; Turner, S. F.; McFiggans, G.; Baltensperger, U. *Geophysical Research Letters* **2008**, *35*.

(68) Swietlicki, E.; Hansson, H. C.; Hameri, K.; Svenningsson, B.; Massling, A.; McFiggans, G.; McMurry, P. H.; Petaja, T.; Tunved, P.; Gysel, M.; Topping, D.; Weingartner, E.; Baltensperger, U.; Rissler, J.; Wiedensohler, A.; Kulmala, M. *Tellus Series B-Chemical and Physical Meteorology* **2008**, *60*, 432.

- (69) Duplissy, J.; Gysel, M.; Sjogren, S.; Meyer, N.; Good, N.; Kammermann, L.; Michaud, V.; Weigel, R.; dos Santos, S. M.; Gruening, C.; Villani, P.; Laj, P.; Sellegri, K.; Metzger, A.; McFiggans, G. B.; Wehrle, G.; Richter, R.; Dommen, J.; Ristovski, Z.; Baltensperger, U.; Weingartner, E. *Atmos. Meas. Tech.* **2009**, *2*, 363.
- (70) Suess, D. T.; Prather, K. A. *Chemical Reviews* **1999**, *99*, 3007.
- (71) Prather, K. A.; Hatch, C. D.; Grassian, V. H. *Annual Review of Analytical Chemistry* **2008**, *1*, 485.
- (72) Noble, C. A.; Prather, K. A. *Mass Spectrom. Rev.* **2000**, *19*, 248.
- (73) Walser, M. L.; Desyaterik, Y.; Laskin, J.; Laskin, A.; Nizkorodov, S. A. *PCCP* **2008**, *10*, 1009.
- (74) Walser, M. L.; Park, J.; Gomez, A. L.; Russell, A. R.; Nizkorodov, S. A. *J. Phys. Chem. A* **2007**, *111*, 1907.
- (75) Jayne, J. T.; Leard, D. C.; Zhang, X.; Davidovits, P.; Smith, K. A.; Kolb, C. E.; Worsnop, D. R. *Aerosol Science and Technology* **2000**, *33*, 49:70.
- (76) Heaton, K. J.; Dreyfus, M. A.; Wang, S.; Johnston, M. V. *Environmental Science & Technology* **2007**, *41*, 6129.
- (77) Heaton, K. J.; Sleighter, R. L.; Hatcher, P. G.; Hall Iv, W. A.; Johnston, M. V. *Environmental Science & Technology* **2009**, *43*, 7797.
- (78) Jimenez, J. L.; Canagaratna, M. R.; Donahue, N. M.; Prevot, A. S. H.; Zhang, Q.; Kroll, J. H.; DeCarlo, P. F.; Allan, J. D.; Coe, H.; Ng, N. L.; Aiken, A. C.; Docherty, K. S.; Ulbrich, I. M.; Grieshop, A. P.; Robinson, A. L.; Duplissy, J.; Smith, J. D.; Wilson, K. R.; Lanz, V. A.; Hueglin, C.; Sun, Y. L.; Tian, J.; Laaksonen, A.; Raatikainen, T.; Rautiainen, J.; Vaattovaara, P.; Ehn, M.; Kulmala, M.; Tomlinson, J. M.; Collins, D. R.; Cubison, M. J.; E.; Dunlea, J.; Huffman, J. A.; Onasch, T. B.; Alfarra, M. R.; Williams, P. I.; Bower, K.; Kondo, Y.; Schneider, J.; Drewnick, F.; Borrmann, S.; Weimer, S.; Demerjian, K.; Salcedo, D.; Cottrell, L.; Griffin, R.; Takami, A.; Miyoshi, T.; Hatakeyama, S.; Shimono, A.; Sun, J. Y.; Zhang, Y. M.; Dzepina, K.; Kimmel, J. R.; Sueper, D.; Jayne, J. T.; Herndon, S. C.; Trimborn, A. M.; Williams, L. R.; Wood, E. C.; Middlebrook, A. M.; Kolb, C. E.; Baltensperger, U.; Worsnop, D. R. *Science* **2009**, *326*, 1525.
- (79) Aiken, A. C.; Decarlo, P. F.; Kroll, J. H.; Worsnop, D. R.; Huffman, J. A.; Docherty, K. S.; Ulbrich, I. M.; Mohr, C.; Kimmel, J. R.; Sueper, D.; Sun, Y.; Zhang, Q.; Trimborn, A.; Northway, M.; Ziemann, P. J.; Canagaratna, M. R.; Onasch, T. B.; Alfarra, M. R.; Prevot, A. S. H.; Dommen, J.; Duplissy, J.; Metzger, A.; Baltensperger, U.; Jimenez, J. L. *Environmental Science & Technology* **2008**, *42*, 4478.
- (80) Ebben, C. J.; Martinez, I. S.; Shrestha, M.; Buchbinder, A.; Corrigan, A. L.; Guenther, A.; Karl, T.; Petaejae, T.; Song, W. W.; Zorn, S. R.; Artaxo, P.; Kulmala, M.; Martin, S. T.; Russell, L. M.; Williams, J.; Geiger, F. M. *ACP* **2011**, *11*, 10317.
- (81) Frosch, M.; Bilde, M.; DeCarlo, P. F.; Juranyi, Z.; Tritscher, T.; Dommen, J.; Donahue, N. M.; Gysel, M.; Weingartner, E.; Baltensperger, U. *Journal of Geophysical Research-Atmospheres* **2011**, *116*.
- (82) King, S. M.; Rosenoern, T.; Shilling, J. E.; Chen, Q.; Martin, S. T. *Geophysical Research Letters* **2007**, *34*.
- (83) Kuwata, M.; Chen, Q.; Martin, S. T. *Physical Chemistry Chemical Physics* **2011**, *13*, 14571.

- (84) Lee, B. H.; Pierce, J. R.; Engelhart, G. J.; Pandis, S. N. *Atmospheric Environment* **2011**, *45*, 2443.
- (85) Shilling, J. E.; Chen, Q.; King, S. M.; Rosenoern, T.; Kroll, J. H.; Worsnop, D. R.; DeCarlo, P. F.; Aiken, A. C.; Sueper, D.; Jimenez, J. L.; Martin, S. T. *Atmospheric Chemistry and Physics* **2009**, *9*, 771.
- (86) Shilling, J. E.; Chen, Q.; King, S. M.; Rosenoern, T.; Kroll, J. H.; Worsnop, D. R.; McKinney, K. A.; Martin, S. T. *Atmospheric Chemistry and Physics* **2008**, *8*, 2073.
- (87) Stanier, C. O.; Pathak, R. K.; Pandis, S. N. *Environmental Science & Technology* **2007**, *41*, 2756.
- (88) Wang, J.; Doussin, J. F.; Perrier, S.; Perraudin, E.; Katrib, Y.; Pangu, E.; Picquet-Varrault, B. *Atmos. Meas. Tech.* **2011**, *4*, 2465.
- (89) George, I. J.; Abbatt, J. P. D. *Atmospheric Chemistry and Physics* **2010**, *10*, 5551.
- (90) Nojgaard, J. K.; Norgaard, A. W.; Wolkoff, P. *Atmospheric Environment* **2007**, *41*, 8345.
- (91) Rohr, A. C.; Weschler, C. J.; Koutrakis, P.; Spengler, J. D. *Aerosol Science and Technology* **2003**, *37*, 65.
- (92) Tolocka, M. P.; Heaton, K. J.; Dreyfus, M. A.; Wang, S. Y.; Zordan, C. A.; Saul, T. D.; Johnston, M. V. *Environmental Science & Technology* **2006**, *40*, 1843.
- (93) Gao, Y. Q.; Hall, W. A.; Johnston, M. V. *Environmental Science & Technology* **2010**, *44*, 7897.
- (94) Chow, J. C.; Yu, J. Z.; Watson, J. G.; Ho, S. S. H.; Bohannon, T. L.; Hays, M. D.; Fung, K. K. *Journal of Environmental Science and Health Part a-Toxic/Hazardous Substances & Environmental Engineering* **2007**, *42*, 1521.
- (95) Laj, P.; Klausen, J.; Bilde, M.; Plass-Duelmer, C.; Pappalardo, G.; Clerbaux, C.; Baltensperger, U.; Hjorth, J.; Simpson, D.; Reimann, S.; Coheur, P. F.; Richter, A.; De Maziere, M.; Rudich, Y.; McFiggans, G.; Torseth, K.; Wiedensohler, A.; Morin, S.; Schulz, M.; Allan, J. D.; Attie, J. L.; Barnes, I.; Birmili, W.; Cammas, J. P.; Dommen, J.; Dorn, H. P.; Fowler, D.; Fuzzi, S.; Glasius, M.; Granier, C.; Hermann, M.; Isaksen, I. S. A.; Kinne, S.; Koren, I.; Madonna, F.; Maione, M.; Massling, A.; Moehler, O.; Mona, L.; Monks, P. S.; Mueller, D.; Mueller, T.; Orphal, J.; Peuch, V. H.; Stratmann, F.; Tanre, D.; Tyndall, G.; Riziq, A. A.; Van Roozendaal, M.; Villani, P.; Wehner, B.; Wex, H.; Zardini, A. A. *Atmos. Environ.* **2009**, *43*, 5351.
- (96) Docherty, K. S.; Wu, W.; Lim, Y. B.; Ziemann, P. J. *Environmental Science & Technology* **2005**, *39*, 4049.
- (97) Tobias, H. J.; Ziemann, P. J. *Analytical Chemistry* **1999**, *71*, 3428.
- (98) Pratt, K. A.; Prather, K. A. *Mass Spectrom. Rev.* **2012**, *31*, 1.
- (99) Schnelle-Kreis, J.; Orasche, J.; Abbaszade, G.; Schaefer, K.; Harlos, D. P.; Hansen, A. D. A.; Zimmermann, R. *Analytical and Bioanalytical Chemistry* **2011**, *401*, 3083.
- (100) Bateman, A. P.; Nizkorodov, S. A.; Laskin, J.; Laskin, A. *Physical Chemistry Chemical Physics* **2009**, *11*, 7931.
- (101) Bateman, A. P.; Walser, M. L.; Desyaterik, Y.; Laskin, J.; Laskin, A.; Nizkorodov, S. A. *Environmental Science & Technology* **2008**, *42*, 7341.

- (102) Laskin, J.; Laskin, A.; Roach, P. J.; Slysz, G. W.; Anderson, G. A.; Nizkorodov, S. A.; Bones, D. L.; Nguyen, L. Q. *Analytical Chemistry* **2010**, *82*, 2048.
- (103) Schwier, A. N.; Sareen, N.; Mitroo, D.; Shapiro, E. L.; McNeill, V. F. *Env. Sci. Technol.* **2010**, *44*, 6174.
- (104) Takahama, S.; Liu, S.; Russell, L. M. *Journal of Geophysical Research-Atmospheres* **2010**, *115*.
- (105) Russell, L. M.; Bahadur, R.; Ziemann, P. J. *Proceedings of the National Academy of Sciences of the United States of America* **2011**, *108*, 3516.
- (106) Duarte, R.; Duarte, A. C. *Trac-Trends Anal. Chem.* **2011**, *30*, 1659.
- (107) Prenni, A. J.; Petters, M. D.; Kreidenweis, S. M.; Heald, C. L.; Martin, S. T.; Artaxo, P.; Garland, R. M.; Wollny, A. G.; Poschl, U. *Nat. Geosci.* **2009**, *2*, 401.
- (108) Poeschl, U.; Martin, S. T.; Sinha, B.; Chen, Q.; Gunthe, S. S.; Huffman, J. A.; Borrmann, S.; Farmer, D. K.; Garland, R. M.; Helas, G.; Jimenez, J. L.; King, S. M.; Manzi, A.; Mikhailov, E.; Pauliquevis, T.; Petters, M. D.; Prenni, A. J.; Roldin, P.; Rose, D.; Schneider, J.; Su, H.; Zorn, S. R.; Artaxo, P.; Andreae, M. O. *Science* **2010**, *329*, 1513.
- (109) Bertram, A. K.; Martin, S. T.; Hanna, S. J.; Smith, M. L.; Bodsworth, A.; Q., C.; M., K.; Liu, A.; Zorn, S. R. *Atmos. Chem. Phys.* **2011**.
- (110) Liu, S.; Takahama, S.; Russell, L. M.; Gilardoni, S.; Baumgardner, D. *Atmospheric Chemistry and Physics* **2009**, *9*, 6849.
- (111) Gilham, R. J. J.; Spencer, S. J.; Butterfield, D.; Seah, M. P.; Quincey, P. G. *Atmospheric Environment* **2008**, *42*, 3888.
- (112) Virtanen, A.; Joutsensaari, J.; Koop, T.; Kannosto, J.; Yli-Pirila, P.; Leskinen, J.; Makela, J. M.; Holopainen, J. K.; Poschl, U.; Kulmala, M.; Worsnop, D. R.; Laaksonen, A. *Nature* **2010**, *467*, 824.
- (113) Takahama, S.; Gilardoni, S.; Russell, L. M.; Kilcoyne, A. L. D. *Atmos. Environ.* **2007**, *41*, 9435.
- (114) Holmes, N. S. *Atmos. Environ.* **2007**, *41*, 2183.
- (115) Zhu, X. D.; Suhr, H. J.; Shen, Y. R. *J. Opt. Soc. America B-Optical Physics* **1986**, *3*, P252.
- (116) Geiger, F. M. *Annu. Rev. Phys. Chem.* **2009**, *60*, 61.
- (117) Konek, C. T.; Musorrafiti, M. J.; Al-Abadleh, H. A.; Bertin, P. A.; Nguyen, S. T.; Geiger, F. M. *J. Am. Chem. Soc.* **2004**, *126*, 11754.
- (118) Voges, A. B.; Al-Abadleh, H. A.; Geiger, F. M. In *Environmental Catalysis*; Grassian, V. H., Ed.; CRC Press: Boca Raton, FL, 2005.
- (119) Voges, A. B. A.-A., H. A.; Geiger, F. M. In *Environmental Catalysis*; Grassian, V., Ed.; CRC Press: Boca Raton, 2005.
- (120) Voges, A. B.; Stokes, G. Y.; Gibbs-Davis, J. M.; Lettan, R. B.; Bertin, P. A.; Pike, R. C.; Nguyen, S. T.; Scheidt, K. A.; Geiger, F. M. *Invited Feature Article in J. Phys. Chem. C* **2007**, *111*, 1567.
- (121) Stokes, G. Y.; Buchbinder, A. M.; Gibbs-Davis, J. M.; Scheidt, K. A.; Geiger, F. M. *Vibrational Spectroscopy* **2009**, *50*, 86.
- (122) Stokes, G. Y.; Chen, E. H.; Buchbinder, A. M.; Geiger, F. M. *in press J. Am. Chem. Soc.* **2009**.
- (123) Stokes, G. Y.; Chen, E. H.; Walter, S. R.; Geiger, F. M. *Journal of Physical Chemistry A* **2009**, *113*, 8985.

- (124) Richmond, G. L. *Annual Review of Physical Chemistry* **2001**, *52*, 357.
- (125) Scatena, L. F.; Brown, M. G.; Richmond, G. L. *Science* **2001**, *292*, 908.
- (126) Shen, Y. R.; Ostroverkhov, V. *Chem. Rev.* **2006**, *106*, 1140.
- (127) Gopalakrishnan, S.; Liu, D.; Allen, H. C.; Kuo, M.; Shultz, M. J. *Chemical Reviews* **2006**, *106*, 1155.
- (128) Liu, D. F.; Ma, G.; Levering, L. M.; Allen, H. C. *Journal of Physical Chemistry B* **2004**, *108*, 2252.
- (129) Mucha, M.; Frigato, T.; Levering, L. M.; Allen, H. C.; Tobias, D. J.; Dang, L. X.; Jungwirth, P. *J. Phys. Chem. B.* **2005**, *109*, 7617.
- (130) Voss, L. F.; Bazerbashi, M. F.; Beekman, C. P.; Hadad, C. M.; Allen, H. C. *J. Geophys. Res.* **2007**, *112*, D06209.
- (131) Allen, H. C.; Gragson, D. E.; Richmond, G. L. *J. Phys. Chem. B* **1999**, *103*, 660.
- (132) Tarbuck, T. L.; Richmond, G. L. *J. Am. Chem. Soc.* **2006**, *128*, 3256.
- (133) Richmond, G. L. *Chemical Reviews* **2002**, *102*, 2693.
- (134) Shen, Y. R. *The Principles of Nonlinear Optics*; John Wiley & Sons, Inc.: Hoboken, NJ, 2003.
- (135) Walter, S. R.; Geiger, F. M. *The Journal of Physical Chemistry Letters* **2009**, *1*, 9.
- (136) Buchbinder, A. M.; Ray, N. A.; Lu, J.; Van Duyne, R. P.; Stair, P. C.; Weitz, E.; Geiger, F. M. *J. AM. Chem. Soc. in press* **2011**.
- (137) Achtyl, J. A.; Geiger, F. A. *Submitted* **2011**.
- (138) Hayes, P. L.; Chen, E. H.; Achtyl, J. L.; Geiger, F. M. *J. Phys. Chem. A* **2009**, *113*, 4269.
- (139) Konek, C. T.; Illg, K. D.; Al-Abadleh, H. A.; Voges, A. B.; Yin, G.; Musorrafiti, M. J.; Schmidt, C. M.; Geiger, F. M. *Journal of the American Chemical Society* **2005**, *127*, 15771.
- (140) Boman, F. C.; Gibbs-Davis, J. M.; Heckman, L. M.; Stepp, B. R.; Nguyen, S. T.; Geiger, F. M. *Journal of the American Chemical Society* **2009**, *131*, 844.
- (141) Wang, H.; Yan, E. C. Y.; Borguet, E.; Eisenthal, K. B. *Chemical Physics Letters* **1996**, *259*, 15.
- (142) Eisenthal, K. B. *Chemical Reviews* **2006**, *106*, 1462.
- (143) Ma, G.; Allen, H. C. *J. Am. Chem. Soc.* **2002**, *124*, 9374.
- (144) de Beer, A. G. F.; Roke, S. *Phys. Rev. B* **2007**, *75*, 245438.
- (145) Dadap, J. I.; de Aguiar, H. B.; Roke, S. *J. Chem. Phys.* **2009**, *130*, 214710.
- (146) Wang, H.; Troxler, T.; Yeh, A.-G.; Dai, H.-L. *Langmuir* **2000**, *16*, 2475.
- (147) Ebben, C. J.; Zorn, S. R.; Lee, S.-B.; Artaxo, P.; Martin, S. T.; Geiger, F. M. *GRL* **2011**, *38*, L16807.
- (148) Martinez, I. S.; Peterson, M. D.; Ebben, C. J.; Hayes, P. L.; Artaxo, P.; Martin, S. T.; Geiger, F. M. *PCCP* **2011**, *13*, 12114.
- (149) Esenturk, O.; Walker, R. A. *J. Phys. Chem. B* **2004**, *108*, 10631.
- (150) *Handbook of Chemistry and Physics: A Ready-Reference Book of Chemical and Physical Data*; 78 ed.; CRC Press, Inc.: Boca Raton, Florida, 1997.
- (151) Buchbinder, A. M.; Weitz, E.; Geiger, F. M. *The Journal of Physical Chemistry C* **2010**, *114*, 554.

- (152) Chen, C. Y.; Even, M. A.; Wang, J.; Chen, Z. *Macromolecules* **2002**, *35*, 9130.
- (153) Opdahl, A.; Phillips, R. A.; Somorjai, G. A. *J. Phys. Chem. B* **2002**, *106*, 5212.
- (154) Miranda, P. B.; Shen, Y. R. *J. Phys. Chem. B* **1999**, *103*, 3292.
- (155) Stokes, G. Y.; Chen, E. H.; Buchbinder, A. M.; Geiger, F. M. *J. Am. Chem. Soc.* **2009**, *131*, 13733.
- (156) Phillips, M. A.; Wildung, M. R.; Williams, D. C.; Hyatt, D. C.; Croteau, R. *Arch. Biochem. Biophys.* **2003**, *411*, 267.
- (157) Ellison, G. B.; Tuck, A. F.; Vaida, V. *J. Geophys. Res.* **1999**, *104*, 11633.
- (158) Oberbeck, V. R.; Marshall, J.; Shen, T. *J. Molec. Evol.* **1991**, *32*, 296.
- (159) Colombo, L. M.; Thomas, R. M.; Luisi, P. L. *Chirality* **1991**, *3*, 233.
- (160) Yassaa, N.; Williams, J. *Atmos. Env.* **2005**, *39*, 4875.
- (161) Williams, J.; Yassaa, N.; Bartenbach, S.; Lelieveld, J. *ACP* **2007**, *7*, 973.
- (162) Armstrong, D. W.; Kullman, J. P.; Chen, X. H.; Rowe, M. *Chirality* **2001**, *13*, 153.
- (163) Salma, I.; Meszaros, T.; Maenhaut, W.; Vass, E.; Majer, Z. *Atmos. Chem. Phys.* **2010**, *10*, 1315.
- (164) Noziere, B.; Gonzalez, N. J. D.; Borg-Karlson, A.-K.; Pei, Y.; Redeby, J. P.; Krejci, R.; Dommen, J.; Prevot, A. S. H.; Anthonsen, T. *Geophysical Research Letters* **2011**, *38*.
- (165) Boyd, R. W. *Nonlinear Optics*; Academic Press: New York, 2003.
- (166) Poeschl, U.; Martin, S. T.; Sinha, B.; Chen, Q.; Gunthe, S. S.; Huffman, J. A.; Borrmann, S.; Farmer, D. K.; Garland, R. M.; Helas, G.; Jimenez, J. L.; King, S. M.; Manzi, A.; Mikhailov, E.; Pauriquevis, R.; Petters, M. D.; Prenni, A. J.; Roldin, P.; Rose, D.; Schneider, J.; Su, H.; Zorn, S. R.; Artaxo, P. A., M. O. *Science* **2010**, *329*, 1513.
- (167) Paulot, F.; Crouse, J. D.; Kjaergaard, H. G.; Kv^orten, A.; St. Clair, J. M.; Seinfeld, J. H.; Wennberg, P. O. *Science* **2009**, *325*, 730.
- (168) Claeys, M.; Graham, B.; Vas, G.; Vermeylen, R.; Pashynska, V.; Cafmeyer, J.; Guyon, P.; Andreae, M. O.; Artaxo, P.; Maenhaut, W. *Science* **2004**, *303*, 1173.
- (169) Jacobson, M. Z. *Geophysical Research Letters* **2000**, *27*, 217.
- (170) Odum, J. R.; Jungkamp, T. P. W.; Griffin, R. J.; Flagan, R. C.; Seinfeld, J. H. *Science* **1997**, *276*, 96.
- (171) Kim, H. D.; Balgar, T.; Hasselbrink, E. *Chem. Phys. Lett.* **2011**, *508*, 1.
- (172) Andrews, A. B.; McClelland, A.; Korkeila, O.; Demidov, A.; Krummel, A.; Mullins, O. C.; Chen, Z. *Langmuir* **2011**, *27*, 6049.
- (173) Karl, T.; Guenther, A.; Yokelson, R. J.; Greenberg, J. P.; Potosnak, M.; Blake, D. R.; Artaxo, P. *JGR* **2007**, *112*, D18302.
- (174) Lelieveld, J.; Butler, T. M.; Crowley, J. N.; Dillon, T. J.; Fischer, H.; Ganzeveld, L.; Harder, H.; Lawrence, M. G.; Martinez, M.; Taraborrelli, D.; Williams, J. *Nature* **2008**, *452*, 737.

List of Figures

Figure 1. Global map of the canopy height of the Earth's forests, with dark green indicating heights of up to 70 m, and field sampling locations indicated (**A**). European field sampling location at Hyytiälä, Finland, North American field sampling location at Blodgett forest, and South American field sampling site at Tower TT34 in the central Amazon Basin (**B**). Figure 1A adapted from http://www.nasa.gov/images/content/470377main_globaltreecanopy_cutoutmap.jpg.

Figure 2. (**A**) Particle Sampler for collecting particles having aerodynamic diameters below 1 μm used in Finland and (**B**) micro-orifice uniform-deposit impactor (MOUDI) used in the Amazon Basin showing the (**left**) first four stages of size separation, the multiple nozzles for the 1.0 μm stage (**top right**), a subset of the MOUDI collecting stages sampled for this work in the central Amazon basin (**bottom right**).

Figure 3. A selection of putative organic molecules thought to be present in secondary organic aerosol particles and corresponding oxygen-to-carbon (O/C) ratios values determined from field intensives in North and South America and Europe, adapted from Jimenez et al. (ref. 78). Vertical lines indicate uncertainties.

Figure 4. Experimental setup used in the vibrational sum frequency generation experiments for studying (**A**) vapor/fused silica and (**B**) filter sample/fused silica interfaces. Reproduced with permission from the European Geosciences Union.

Figure 5. ssp-Polarized SFG spectra of α -pinene vapor in contact with a fused silica window (**A, top**) and α -pinene-derived SOA from the Harvard Environmental Chamber (**A, bottom**). Tapping mode atomic force microscopy images obtained from less than 2 μg of aerosol particle material collected using the PM1 sampler shown in Fig. 2A in

Southern Finland from 6:30AM to 2:00PM on 23 June 2010 (**B**). Simplified cartoon of molecules of interest on the surface of a given aerosol particle collected using the PM1 sampler shown in Fig. 2 (**C**). Red and blue oscillators represent asymmetric and symmetric CH stretches, respectively, of the CH₃ groups.

Figure 6. ssp-Polarized vibrational SFG spectra of a fused silica window in contact with a Teflon filter containing aerosol particles with diameters below 1 μm collected in Southern Finland during the HUMPPA-COPEC 2010 field intensive and corresponding gas phase concentrations of isoprene and α-pinene. **Inset:** Aerodynamic mobility diameter and particle number density recorded during the nucleation event that occurred from 23 to 24 July 2010.

Figure 7. Enantiomeric excess of (+)-α-pinene in the gas phase and corresponding psp-polarized vibrational SFG spectra of aerosol particles collected in the PM1 size range during the times indicated in green, with asterisks marking high EE values associated with advection of emissions from the freshly sawn wood to the field measurement site (**A**). psp- (left) and ssp- (right) polarized SFG spectra obtained from particles collected on 23 (top) and 25 (bottom) March 2011 (**B**).

Figure 8. (**A**) ssp-Polarized SFG spectra of isoprene vapor in contact with fused silica window (top) and of isoprene-derived SOA particles prepared at the Harvard Environmental Chamber (bottom). (**B**) ssp-Polarized SFG spectra of particles having aerodynamic diameter 50% cutoff sizes of 3.2 μm (red) and 1.8 μm (olive) sized particles collected at tower TT34 and of particles having aerodynamic diameter 50% cutoff sizes of (**C**) 1.0 μm (top), 560 nm (middle), and 330 nm (bottom) collected at site TT34 in the central Amazon Basin in March 2008. (**C, right**) Optical images obtained with a 50X

objective and 10X objective as shown in the insets of the bottom five images, along with optical reflectivity spectra obtained from six MOUDI stages containing SOA particles of the indicated aerodynamic size range sampled in the central Amazon basin (**right**).

Figure 9. ssp-Polarized SFG spectra of particles collected during the following dates: 1-4 July 2009 (top), 4-8 July 2009 (second and third from the top), 11-14 July 2009 (fourth from the top), and 25-28 July 2009 (bottom two) in Blodgett Forest, California.

Figure 10. Vibrational SFG spectra in the CH stretching region of aerosol particles from the boreal, tropical, and pine forests discussed in this work.

Table I. Range of concentrations of temperature, relative humidity, OH, O₃, various monoterpenes, and O/C ratio relevant in Southern Finland and the central Amazon Basin.

Species	Southern Finland	Central Amazon	Central California
Temperature [°C]	25 (night) to 32 (day)	22 (night) to 32 (day)	8 (night) to 32 (day)
RH [%]	30–60 (night) to 80–100 (day)	60 (night) to 100 (day)	20-30 (night) to 50-70 (day)
OH [10 ⁶ cm ⁻³]	0.2-3.0	1-3* and 5**	0.04 and 14.67
NO [ppb]	0.1	0.1	0.04-0.17***
O ₃ [ppb]	20-70	1-20	9.7-98.7***
Isoprene [ppb]	0.01-0.70	1-9	0.33-5.79***
α-pinene [ppb]	0.01-1.0	0.01-0.40	0.11-0.61***
β-pinene [ppb]	0.01-0.20	0.008-0.080	0.07-0.35***
Limonene [ppb]	n.a.	0.008-0.080*	n.a.
O/C ratio	0.5-0.7	0.4 +/- 0.1	0.4-0.9

* Data for the same location studied during AMAZE-08 from Karl et al.¹⁷³

** Data for the tropical forest boundary layer from Lelieveld et al.¹⁷⁴

*** Personal communication with R. C. Cohen and E. C. Browne. NO data for 10AM through 6PM; all other data for day and night.

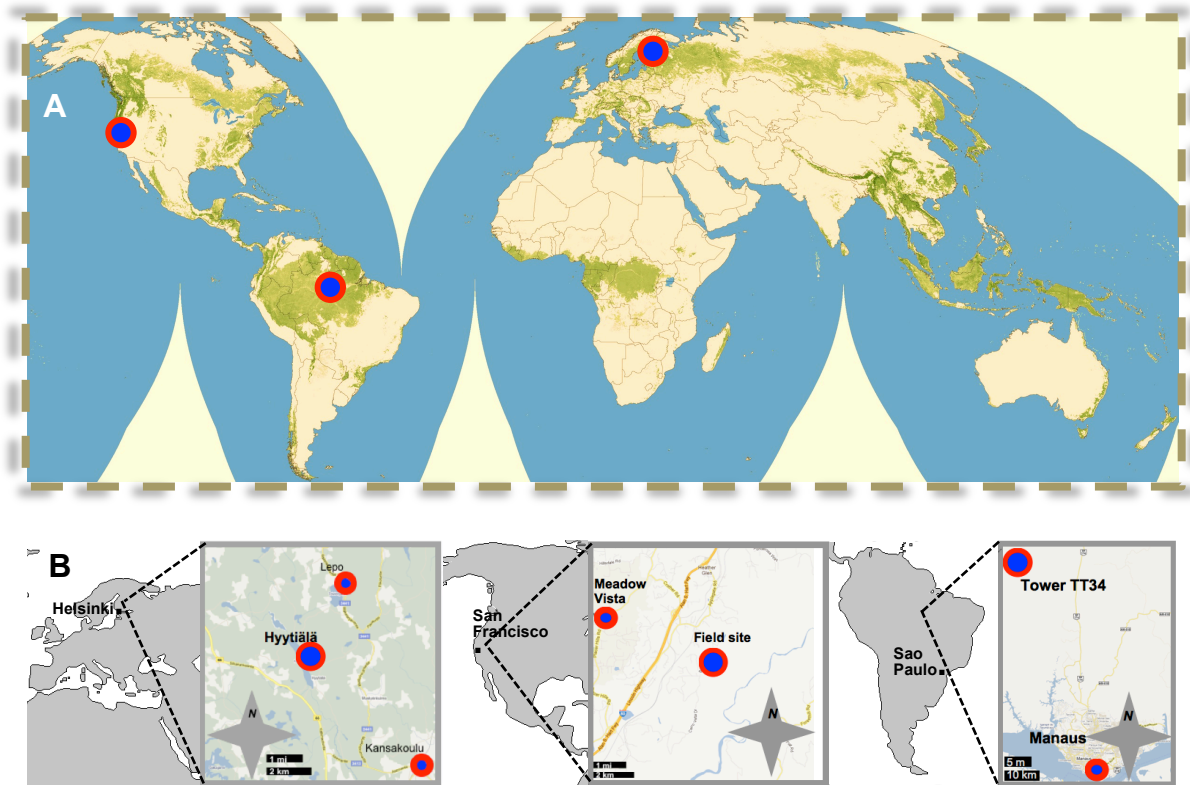


Figure 1.

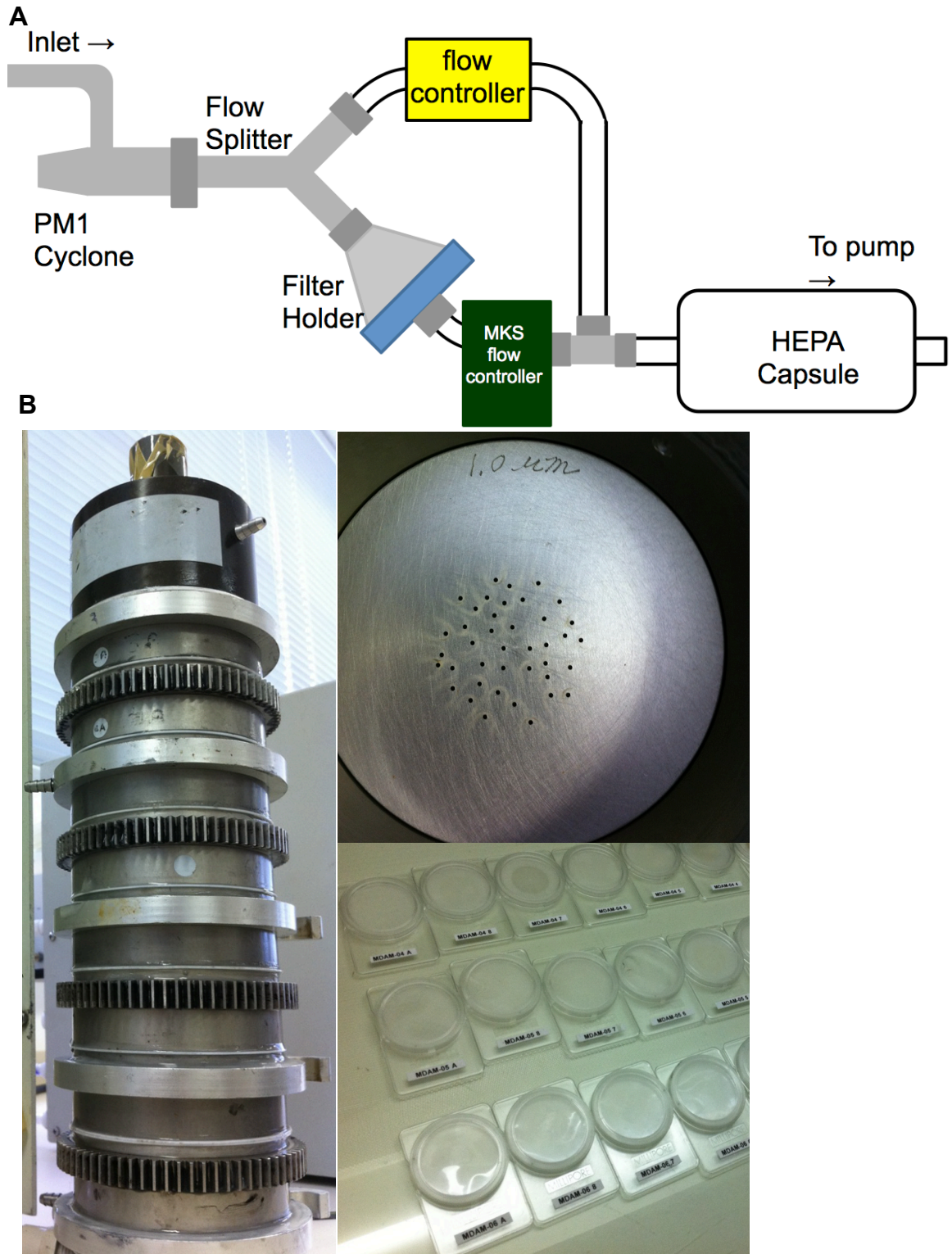


Figure 2.

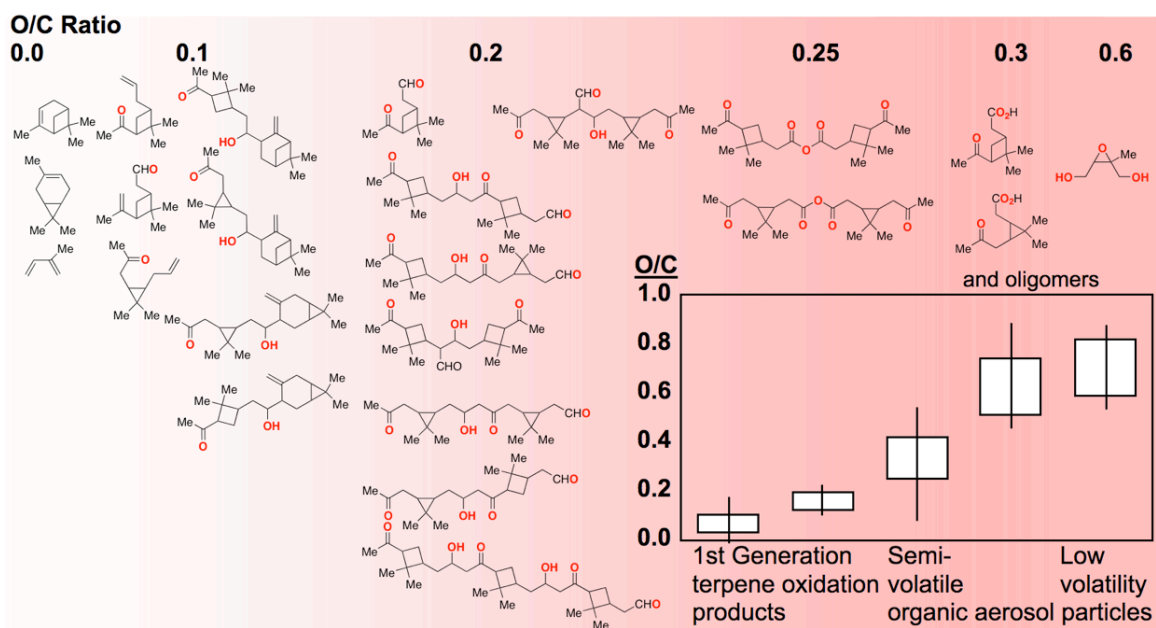


Figure 3.

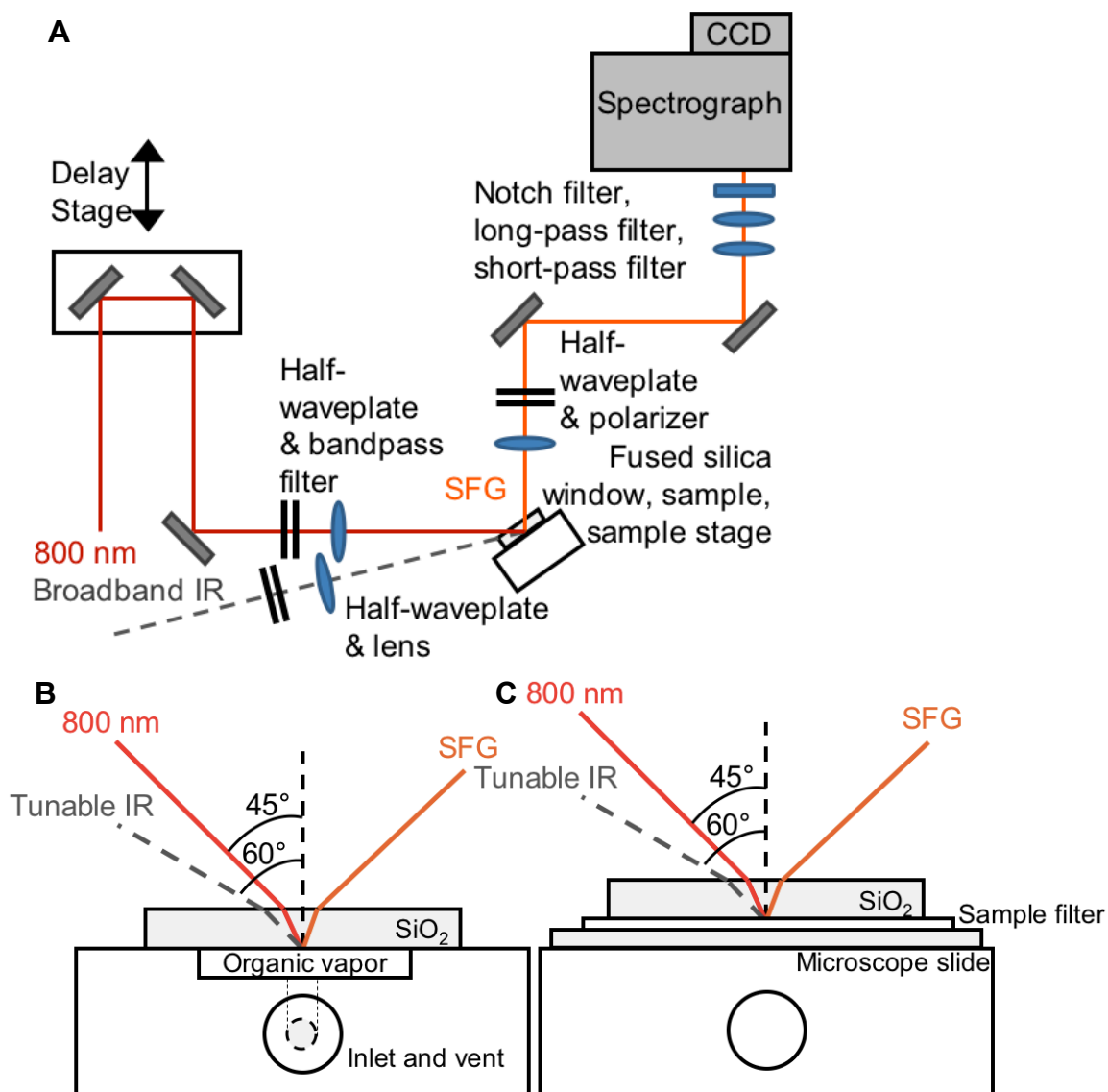


Figure 4.

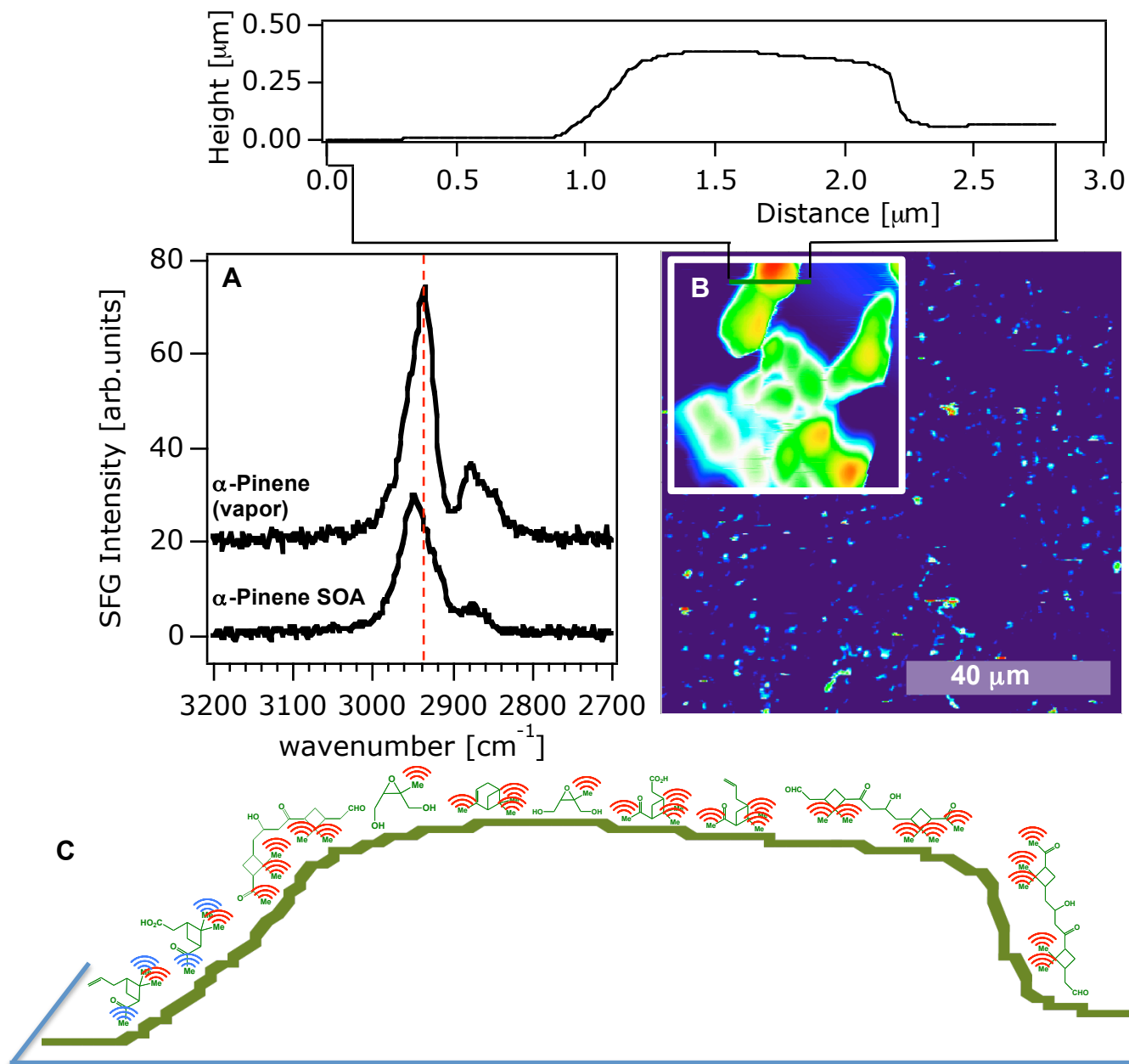


Figure 5.

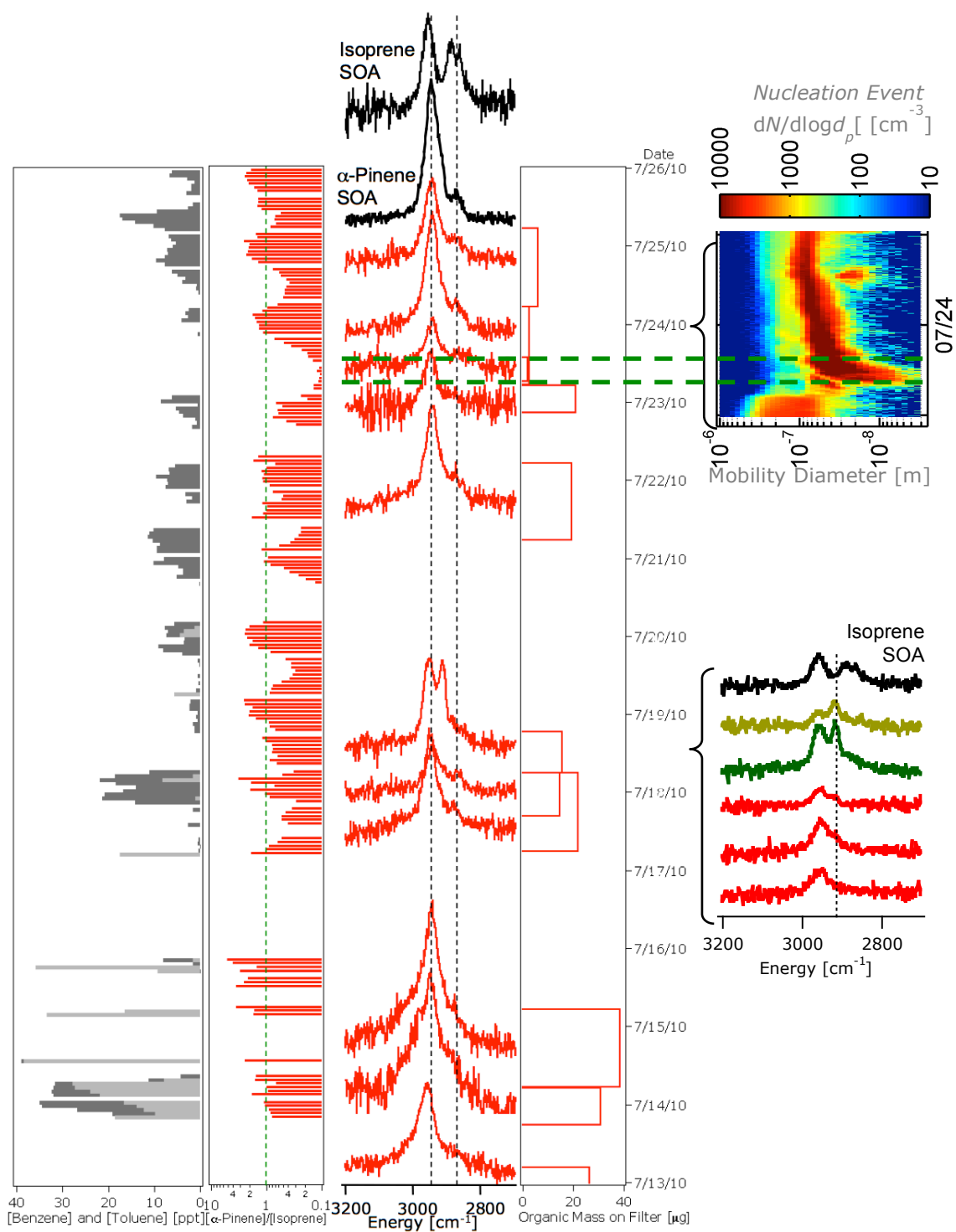


Figure 6

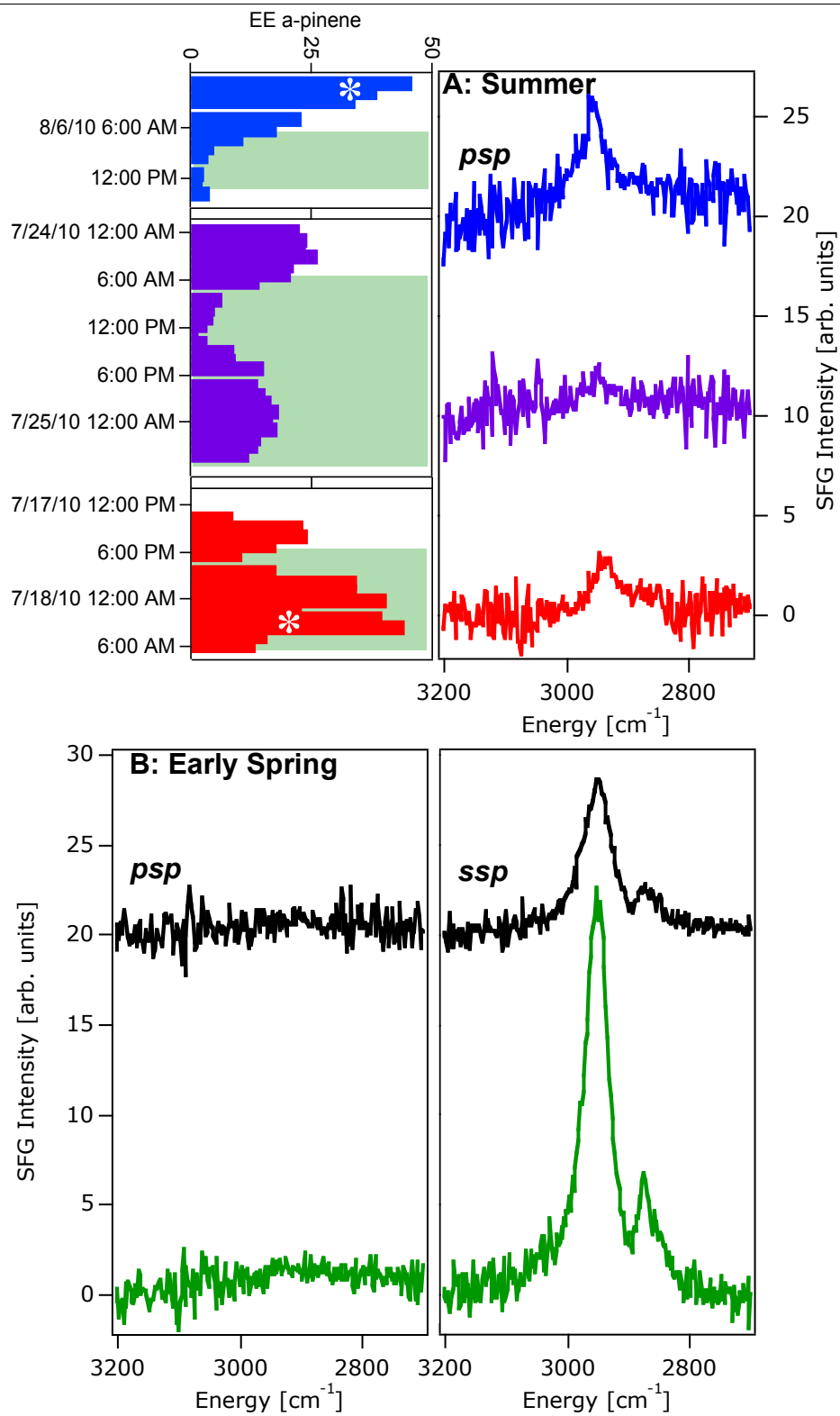


Figure 7

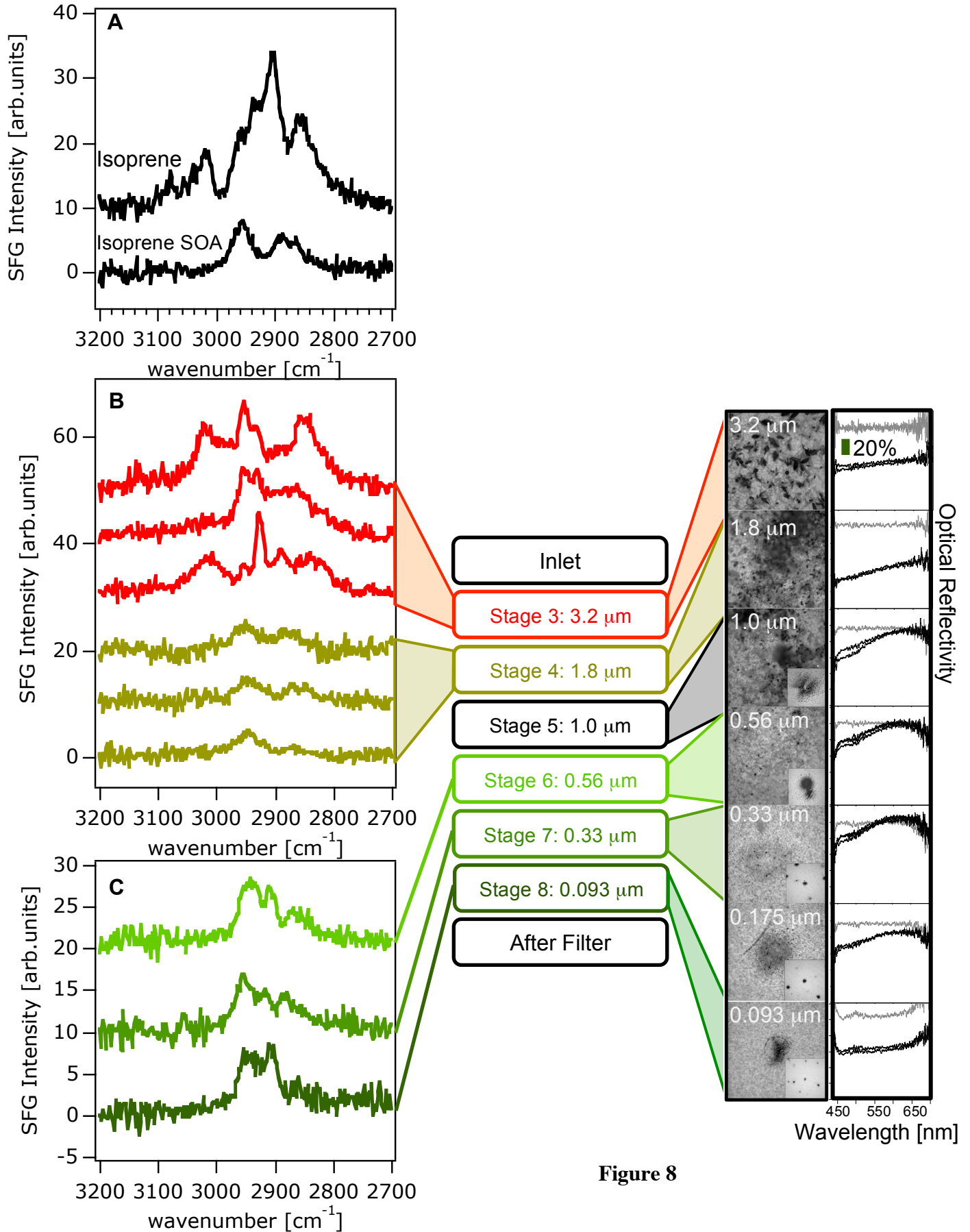
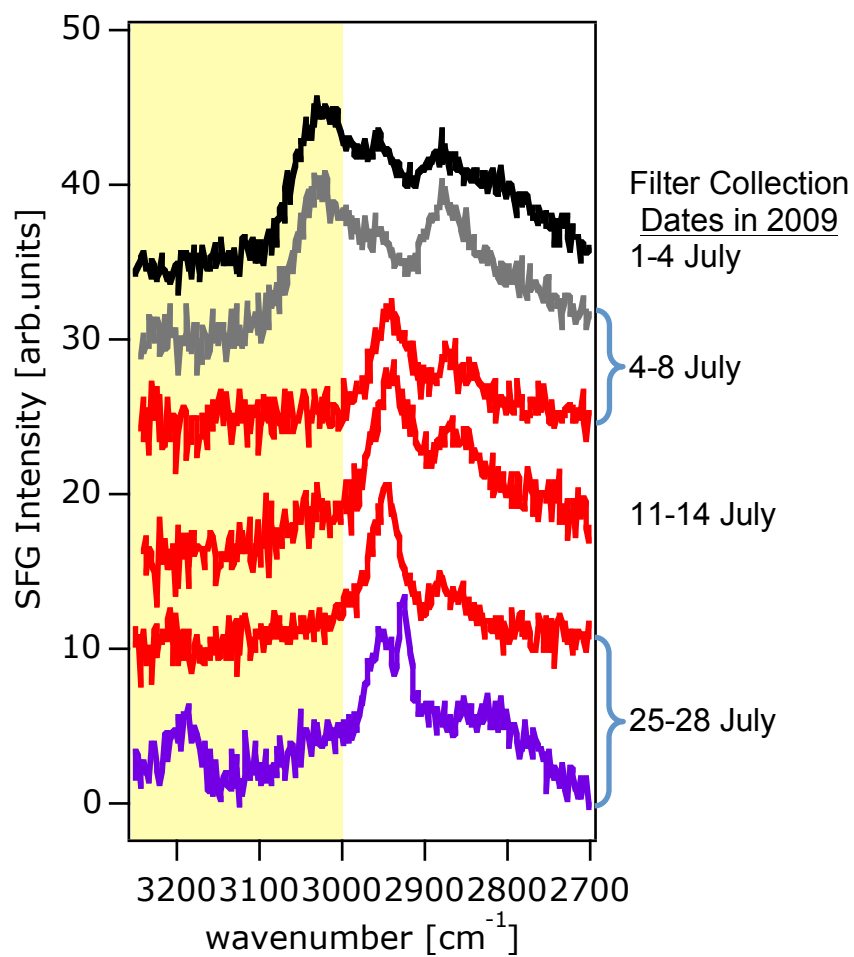


Figure 8

**Figure 9.**

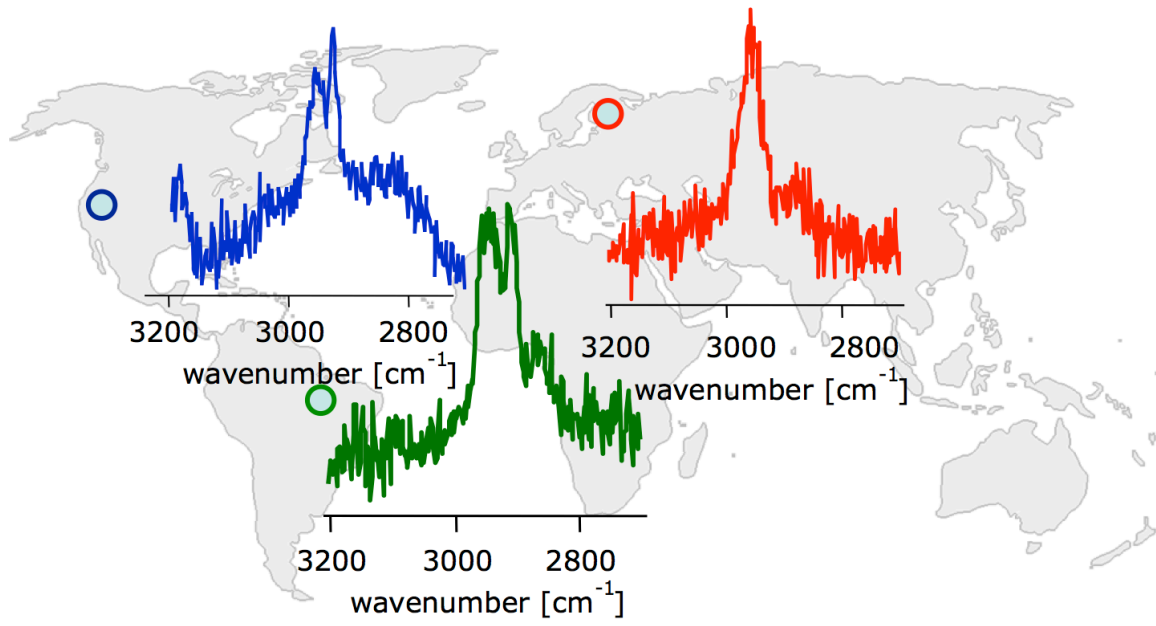


Figure 10.